

UC San Diego

UC San Diego Electronic Theses and Dissertations

Title

Solar Thermochemical Hydrogen Production Plant Design

Permalink

<https://escholarship.org/uc/item/7t26z1mp>

Author

Littlefield, Jesse

Publication Date

2012

Supplemental Material

<https://escholarship.org/uc/item/7t26z1mp#supplemental>

Peer reviewed|Thesis/dissertation

UNIVERSITY OF CALIFORNIA, SAN DIEGO

Solar Thermochemical Hydrogen Production Plant Design

A Thesis submitted in partial satisfaction of the requirements
for the degree Master of Science

in

Chemical Engineering

by

Jesse Littlefield

Committee in charge:

Professor Richard K. Herz, Chair
Professor Pao C. Chau
Professor Jan Talbot

2012

The Thesis of Jesse Littlefield is approved and it is acceptable in quality and form for publication on microfilm and electronically:

Chair

University of California, San Diego

2012

Dedicated to my family and friends

TABLE OF CONTENTS

Signature Page	iii
Dedication	iv
Table of Contents	v
List of Figures	vii
List of Tables	xi
Supplementary Files	xiii
Acknowledgements	xiv
Abstract of the Thesis	xv
Chapter 1: Introduction	1
Footnotes	9
References	9
Chapter 2: Aspen Plus [®] Model Chemistry	11
2.1 General Chemistry	11
2.2 Electrolyte Chemistry	12
2.3 Thermodynamics of Molten Salts	13
References	20
Chapter 3: Aspen Plus [®] Model Methods	21
3.1 Simulations and Flow Sheet Design with Aspen Plus [®]	21
3.2 Tools in Aspen Plus [®] and Their Use in the Flow Sheet	21
3.2.1 Thermodynamic Model ENRTL-SR and Property Input	22
3.2.2 The Gibbs reactor and the Low and High Temperature Reactors	23
3.2.3 The Stoichiometric Reactor and the Mid-Temperature Reactor, Chemical Absorber, and Electrolyzer	24
3.2.4 Design Specification Blocks	26
3.2.5 Calculator Blocks	29
3.2.6 Sensitivity Analyses	31
3.3 Pinch Analysis, Heat Integration, and the MHeatX Block	33
References	43
Chapter 4: Procedure and Error and Warning Analysis	44

Chapter 5: Results and Discussion	48
5.1 Flow Sheet	48
5.2 Energy and Mass Balance	48
5.3 Solar Reactors and the Chemical Absorber	51
5.4 Pinch Analysis and Heat Integration	56
5.5 Power Generation	58
5.6 Values from Design Specifications	60
5.7 Values from Calculator Blocks	62
5.8 Values Obtained from Sensitivity Analyses	64
5.9 Efficiency	66
5.9.1 LHV of Hydrogen	66
5.9.2 Total Heat (Q) and Import Electricity (E)	67
References	73
Chapter 6: Conclusions and Future Work	74
Appendices	77
A. Electrochemical Relations for ELECPOWR FORTRAN Code	77
B. LHV of Hydrogen Conversion Factor	78
C. Complete Stream Tables	79
C.1 Molar Flow Stream Table	79
C.2 Molar Fraction Stream Table	84
C.3 Mass Flow Stream Table	89
C.4 Heat, Pressure, Phase, and Density Stream Table	94
References	99

LIST OF FIGURES

Figure 1.1: Schematic of a sulfur-ammonia thermochemical cycle. Eqs. 1.7, 1.8, and 1.9 occur in the Low-Temp Reactor, Mid-Temp Reactor, and the High-Temp Reactor, respectively. Eq. 1.10 occurs in the Chemical Absorber and Eq. 1.11 occurs in the Electrolytic Reactor	6
Figure 1.2: Simplified schematic of the SA process. Includes reaction occurring in each unit along with reference to the Aspen Plus [®] model name in Figure 1.3 and the equation number in Chapter 1.....	7
Figure 1.3: Flow sheet of the sulfur-ammonia solar thermochemical hydrogen production plant described in the current work.....	8
Figure 2.1: Location of the Chemistry sub-menu in the data browser. Each set of reactions used in the flow sheet is listed here.....	15
Figure 2.2: Location and definition of the reactions which occurred in the chemical absorber as defined in the flow sheet.	15
Figure 2.3: Location and definition of the reactions which occurred in the electrolyzer as defined in the flow sheet.	16
Figure 2.4: Location and definition of the reactions associated with the formation of sulfuric acid.	16
Figure 2.5: Location and definition of the reactions which occurred in the high temperature reactor as defined in the flow sheet.	16
Figure 2.6: Location and definition of the reactions which occurred in the low temperature reactor as defined in the flow sheet.	17
Figure 2.7: Location and definition of the reactions which occurred in the mid-temperature reactor as defined in the flow sheet.	17
Figure 2.8: Example of how the chemistry was defined in the low temperature reactor.	18
Figure 2.9: A list of the components necessary for this process including the components added by the Electrolyte Wizard which is accessed by the button at the bottom of this figure highlighted with a red box.	18
Figure 2.10: Phase diagram of the $K_2SO_4 + K_2S_2O_7$ system at a total pressure of 0.1 MPa [1].	19

Figure 3.1: Location of properties for $(\text{NH}_4)_2\text{SO}_3$, $(\text{NH}_4)_2\text{SO}_4$, K_2SO_4 , and $\text{K}_2\text{S}_2\text{O}_7$ in data browser and the values of the Gibbs energy and enthalpy changes for the respective species.	35
Figure 3.2: Defined phases of the products within the LOTEMRXR RGibbs reactor along with its location in the data browser.	35
Figure 3.3: Location of H2O-MU in the data browser and the definitions of the variables used.	36
Figure 3.4: Shows specification, target, and tolerance for H2O-MU block.	36
Figure 3.5: Shows the manipulated variable and its limits for H2O-MU block.	36
Figure 3.6: Location of SO3CONV in the data browser and the definitions of the variables used.	37
Figure 3.7: Shows specification, target, and tolerance for SO3CONV block.	37
Figure 3.8: Shows the manipulated variable and its limits for SO3CONV block.	37
Figure 3.9: Shows the location of the ELECPOWR calculator in the data browser and the definitions of the variables used.	38
Figure 3.10: Shows the FORTRAN code for ELECPOWR along with its location within the data browser.	38
Figure 3.11: Shows the location of the PLANTEFF calculator in the data browser and the definitions of the variables used.	39
Figure 3.12: Shows the FORTRAN code for PLANTEFF along with its location within the data browser.	39
Figure 3.13: Shows the location of the sensitivity block NH3VAPOR and the definitions of the variables used.	40
Figure 3.14: The temperature of the test heater block was defined as the manipulated variable in NH3VAPOR, ranged from 50 to 150 °C, and incremented by 1 °C.	40
Figure 3.15: Shows how the defined variables were tabulated in NH3PROD.	41
Figure 3.16: Shows the location of the sensitivity block SO3PROD and the definitions of the variables used.	41

Figure 3.17: The temperature of the mid-temperature reactor was defined as the manipulated variable in SO3PROD, ranged from 800 to 850 °C, and incremented by 0.5 °C.....	41
Figure 3.18: Shows how the defined variables were tabulated in SO3PROD.	42
Figure 4.1: Shows how to open the data browser using the highlighted areas. The “Data” menu has the individual options displayed in the data browser window or the “glasses” button can be used to open the data browser window.	46
Figure 4.2: Location of the Control Panel button (left red highlight) and the “Next” button (right red highlight).	46
Figure 4.3: Physical property warning displayed in the control panel for missing dielectric constant (CPDIEC) for SO ₃	46
Figure 4.4: Physical property warning displayed in the control panel. This warning was repeated in 27 occurrences.	46
Figure 4.5: Simulation warning displayed in the control panel for design specification SO3CONV.....	47
Figure 4.6: Simulation warning displayed in the control panel stating zero feed to two blocks in the flow sheet in the beginning of a convergence loop. Also contains the only simulation error displayed in the control panel which also converged in \$SOLVER01 (refer to Figure 4.7).	47
Figure 4.7: \$SOLVER01 converged negating the warnings and error shown in Figure 4.6 and Figure 4.8, respectively. Convergence displayed in the control panel.	47
Figure 5.1: Simplified process flow diagram of the solar thermochemical hydrogen plant. Refer to Table 5.1 for use of Q ₁ – Q ₃ in the energy balance.	68
Figure 5.2: Shifted temperature composite curve generated from a standard pinch analysis procedure where the red line represents the hot streams and the blue line represents the cold streams.	69
Figure 5.3: Non-shifted temperature composite curve generated from a standard pinch analysis procedure where the red line represents the hot streams and the blue line represents the cold streams.	69
Figure 5.4: A grand composite curve generated from a standard pinch analysis procedure.	70

Figure 5.5: Upper results of the NH3VAPOR sensitivity analysis. The peak temperature used was 150 °C and, as shown by the vapor fraction (VAPRFRAC) column, the NH₃/water stream keeps a liquid fraction of 1. 70

Figure 5.6: Intermediate results of the SO3PROD sensitivity analysis. Displays the range of temperatures where the chosen temperature for the mid-temperature reactor of 834.5 °C is located including examples of the temperature ranges that showed a status of errors or warnings. The column FSO3 is the flow of SO₃, column T is the temperature of the mid-temperature reactor, and column FH2 is the flow of product H₂. 71

Figure 5.7: Plot of the sensitivity analysis SO3PROD showing the mass flow rate of SO₃ [kg/hr] versus the temperature of the mid-temperature reactor. 72

LIST OF TABLES

Table 2.1: Stoichiometric results of the Electrolyte Wizard.	12
Table 2.2: Thermodynamic parameters $\Delta H^{\circ}_{298.15\text{ K}}$ [J/mol] and $S^{\circ}_{298.15\text{ K}}$ [J/mol·K] for K_2SO_4 and $\text{K}_2\text{S}_2\text{O}_7$ [1].	13
Table 5.1: Energy and mass balance based on the plant design. Refer to Figure 5.1 for definitions of $Q_1 - Q_3$ in the plant.....	49
Table 5.2: Energy and mass balance based on the current work.....	50
Table 5.3: Summary of the low temperature reactor results.....	52
Table 5.4: Mass and energy balance of the low temperature reactor.	52
Table 5.5: Phase composition of the ammonia and molten salt outlet streams of the low temperature reactor.	53
Table 5.6: Summary of the mid-temperature reactor results.....	53
Table 5.7: Mass and energy balance of the mid-temperature reactor.....	54
Table 5.8: VL equilibrium results for the mid-temperature reactor.	54
Table 5.9: Summary of the high temperature reactor results.	54
Table 5.10: Mass and energy balance of the high temperature reactor.	55
Table 5.11: Phase composition of the outlet stream of the high temperature reactor. .	55
Table 5.12: Summary of the chemical absorber results.	55
Table 5.13: Mass and energy balance of the chemical absorber.	56
Table 5.14: VL equilibrium results for the chemical absorber.....	56
Table 5.15: Input and results of the pinch analysis spreadsheet from [2]. Columns “Stream Name” through “Specific Heat Capacity” were input and the remaining columns were results of the calculations done within the spreadsheet.	57
Table 5.16: Results of the single-flow condensing turbine (TURBINE).	58

Table 5.17: Results of the H2O-MU design specification.	60
Table 5.18: Results of the SO3CONV design specification.....	61
Table 5.19: Results of the ELECPOWR calculator block.....	62
Table 5.20: Summary of the electrolyzer results.....	62
Table 5.21: Mass and energy balance of the electrolyzer.	63
Table 5.22: VL equilibrium results for the electrolyzer.	63
Table 5.23: Results of the PLANTEFF calculator block.	63
Table C.1.1: Molar flow rate stream table including every stream in the process.	80
Table C.2.1: Molar fraction stream table including every stream in the process.	85
Table C.3.1: Mass flow rate stream table including every stream in the process.	90
Table C.4.1: Stream table including temperature, pressure, vapor fraction, liquid fraction, enthalpy, and density of every stream in the process.	95

SUPPLEMENTARY FILES

SA Process.apw

SA Process.bkp

ACKNOWLEDGEMENTS

I would like to acknowledge Professor Richard K. Herz for his unwavering support as my advisor. Without his guidance and seemingly infinite patience, the research and this thesis would not have been possible and I would not have known I could even complete them. I would also like to thank Professor Jan Talbot for her frequent pushes to complete this project. Also the experience she gave me in the past and present that aided in all things necessary to complete this project. And last, the discussions that showed insight to complete the work.

Dr. Lloyd C. Brown was an invaluable source of information during my work and without the discussions we had, my work wouldn't have progressed to the end result.

This work was funded by the Hydrogen and Fuel Cells Program under the Department of Energy's Efficiency and Renewable Energy program through a subcontract with SAIC. I would also like to acknowledge the other groups associated with this project: Electrosynthesis Company, Inc., Thermochemical Engineering (TChemE) Solutions, and the University of California, San Diego.

Lastly, I would like to acknowledge fellow graduate students working on this project Mimi Wang and Wesley Luc for their discussions and support.

ABSTRACT OF THE THESIS

Solar Thermochemical Hydrogen Production Plant Design

by

Jesse Littlefield

Master of Science in Chemical Engineering

University of California, San Diego, 2012

Professor Richard K. Herz, Chair

A plant was designed that uses a solar sulfur-ammonia thermochemical water-splitting cycle for the production of hydrogen. Hydrogen is useful as a fuel for stationary and mobile fuel cells. The chemical process simulator Aspen Plus® was used to model the plant and conduct simulations. The process utilizes the electrolytic oxidation of aqueous ammonium sulfite in the hydrogen production half cycle and the thermal decomposition of molten potassium pyrosulfate and gaseous sulfur trioxide in the oxygen production half cycle. The reactions are driven using solar thermal energy

captured from a heliostat array focused on a receiver. The plant's feed stream is water and the product streams are hydrogen and oxygen; all other materials are contained within the plant. The model is for full-scale operation that would generate 133,333 kg of hydrogen per day, which is equivalent to 370 MW on a lower heating value basis. Thermodynamic properties of chemical species obtained from literature, and from laboratory experiments conducted in another part of this project, were entered into the model to improve its accuracy. Design specifications were placed in strategic areas of the model to aid in its convergence. Model convergence is challenging to obtain because of the many material and energy recycle loops within the plant. Calculator blocks were used to obtain power requirements for the electrolyzer and efficiencies of the entire plant based on definitions from the Department of Energy, which funded this project. Results from this work will aid in the design of a large-scale hydrogen production plant.

Chapter 1: Introduction

There are many political, economic, and environmental issues concerning the use of fossil fuels. Because of these problems, research into a sustainable, environmentally friendly source of fuel that can be manufactured has become prevalent. There are many areas of study on sources of sustainable energy including hydroelectric, wind, geothermal, biomass, solar photovoltaic, and solar-thermal [1], each having its own advantages and disadvantages. The current work focuses on solar-thermal energy storage where the thermal energy from the sun is stored as hydrogen.

Hydrogen has received a lot of attention because of its abundance, particularly in water, and that the product of its use is only water. If the hydrogen can be produced with low or zero CO₂ emissions, this would only add to its environmental compatibility. The hydrogen produced can be used in several areas. These areas include petroleum processing, petrochemical production, oil and fat hydrogenation, fertilizer production, metallurgical applications such as the production of nickel, and the electronics industry in the epitaxial growth of polysilicon [2]. However, there is also significant use of hydrogen in fuel cells. Fuel cells can be both mobile and stationary. Mobile fuel cells are widely known and have applications in automobiles. Stationary fuel cells are generally used in the residential sector and for industrial applications [3].

The US Department of Energy (DOE) has set a goal of producing 10 quads (1 quad = 10¹⁵ Btu) of hydrogen per year for transportation use from renewable sources

in the years 2030 to 2050 [4]. The DOE has also set the goal of reducing the cost of hydrogen to \$3.00 per gge (gallon of gasoline equivalent) by 2017 [5].

One method of hydrogen production is splitting water, shown by the following reaction



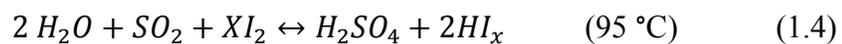
Eq. 1.1 is the thermolysis of water. This is a very energy intensive method to split water and can require temperatures as high as 2500 K [6]. To meet the goals stated previously, the DOE has funded projects to study several thermochemical hydrogen production processes. There are over 800 published water-splitting thermochemical cycles (WSTC), but only a few are economically or technologically feasible [7,8].

One method of water-splitting is the Zn/ZnO cycle. This method of water splitting has been studied thoroughly [9]. It is a two-step process that allows the hydrogen and oxygen to release in different steps as shown in the following reactions



However, there are issues associated with this cycle including temperatures that are comparable to thermolysis and the tendency for Zn and O₂ to recombine leading to either a low H₂ yield or a need of the components separation [10].

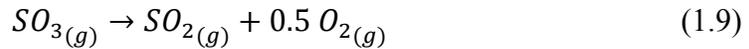
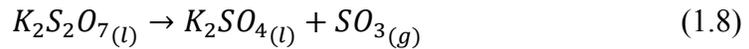
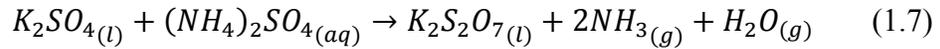
Another WSTC is the sulfur-iodine (S-I) cycle. This is a three-step cycle described by the following reactions



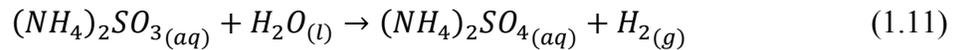
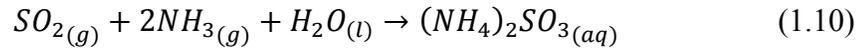
This does not have temperatures above 870 °C making it a competitor to the solid oxide cycles [11]. But because of the high reactivity of sulfur and iodine, complicated separation processes are required [10].

The current work focuses on the sulfur-ammonia (SA) cycle. Figure 1.1 shows a schematic of the SA cycle. This is a five-step, all fluid process. It involves separate hydrogen and oxygen generation half-cycles described by the following equations

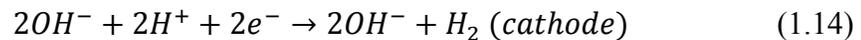
Oxygen Production Half-Cycle:



Hydrogen Production Half-Cycle:



This process was originally based on the Westinghouse cycle and uses both a thermochemical and an electrolytic step [12]. Eq. 1.11 is performed in an electrolytic process described by the following electrolytic half-cell reactions in basic media



The hydroxide ions can be transported through an alkaline anion exchange membrane.

This project must show that the cycle requires lower temperatures than the previously mentioned cycles, use no solids, and must not require costly gas separation.

Aspen Plus[®] chemical process simulator was used to design the flow sheet for this project¹. Figure 1.2 shows a simplified schematic of the SA process while Figure 1.3 is the full and final flow sheet of the current work. The reactions carried out in the low, mid, and high temperature reactors are solar-thermal reactions. The heat required for those reactors is supplied from the heliostat array and solar concentrating tower. The reaction carried out in the absorber is a chemical absorption reaction and the reaction carried out in the electrolyzer is an electrolytic reaction in which the power requirement is supplied by the electricity generating portion of the flow sheet.

Figure 1.3 shows clearly the number of material recycle loops associated with this process. This was a challenge in building the flow sheet because of convergence issues. The sequential modular method of solving the system of equations associated with the flow sheet meant that if there was an issue in one block, it was difficult to converge the entire process.

This research focuses on the design of the process flow sheet for accurate simulation of the SA cycle in a production plant. Chapter 2 is the background and describes more about the current research. Chapter 3 describes how Aspen Plus[®] was used and the tools used to create the final flow sheet. Chapter 4 describes how to use the final flow sheet and analyzes any warnings and/or errors that occurred after running the simulation. Chapter 5 lists the results of the simulation and Chapter 6 is the conclusion and recommendations for future work.

The current work on the sulfur-ammonia solar thermochemical hydrogen (STCH) production plant simulation in Aspen Plus[®] is based on previous work by the Florida Solar Energy Center (FSEC). FSEC developed a flow sheet that was used as a

starting point for the current work. FSEC was also funded through the DOE and worked closely with SAIC. The current work developed a new Aspen Plus[®] model. Refer to [13] and [14] for more information on the work FSEC had accomplished before the University of California, San Diego began the current research.

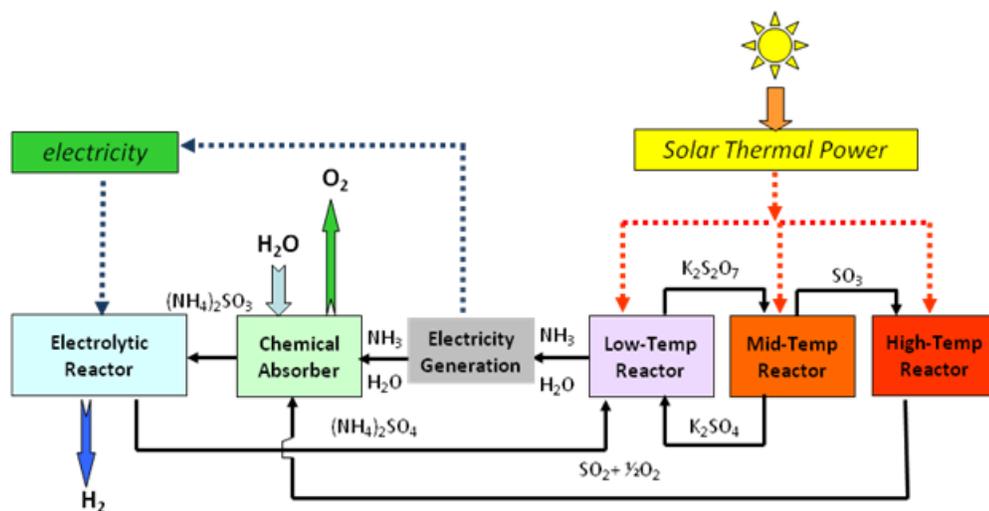
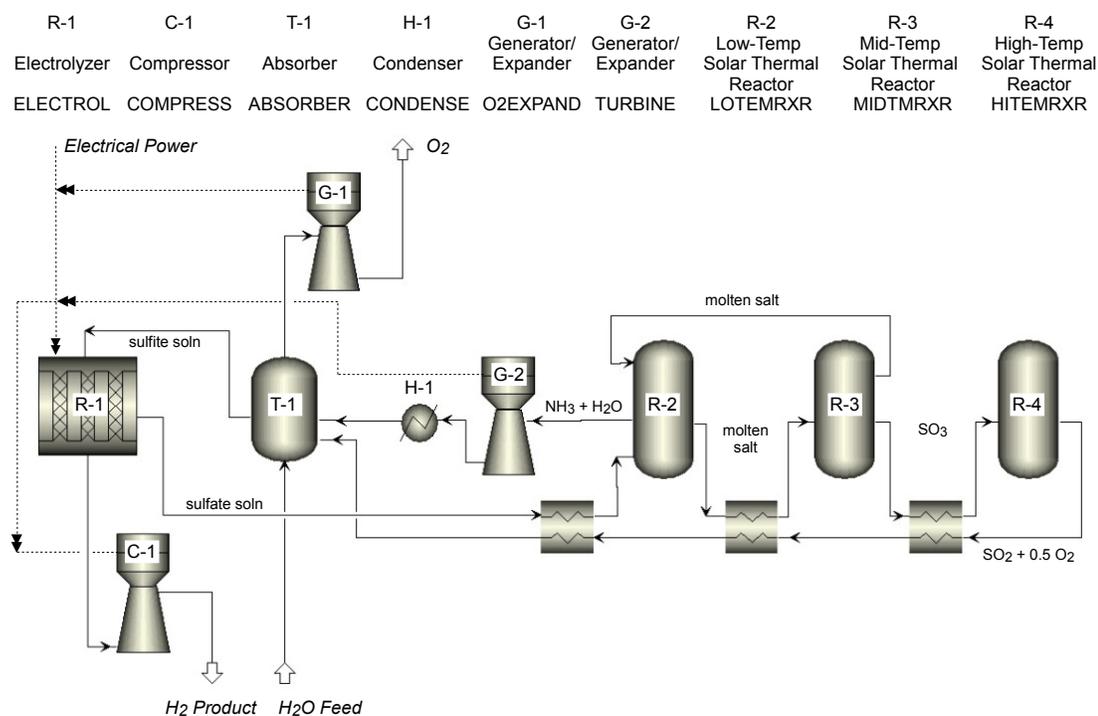


Figure 1.1: Schematic of a sulfur-ammonia thermochemical cycle. Eqs. 1.7, 1.8, and 1.9 occur in the Low-Temp Reactor, Mid-Temp Reactor, and the High-Temp Reactor, respectively. Eq. 1.10 occurs in the Chemical Absorber and Eq. 1.11 occurs in the Electrolytic Reactor.



Unit	Aspen Plus® Model Name	Reaction	Eq. (#)
R-1	ELECTROL	$(NH_4)_2SO_3(aq) + H_2O(l) \rightarrow (NH_4)_2SO_4(aq) + H_2(g)$	(1.11)
T-1	ABSORBER	$SO_2(g) + 2NH_3(g) + H_2O(l) \rightarrow (NH_4)_2SO_3(aq)$	(1.10)
R-2	LOTEMRXR	$K_2SO_4(l) + (NH_4)_2SO_4(aq) \rightarrow K_2S_2O_7(l) + 2NH_3(g) + H_2O(g)$	(1.7)
R-3	MIDTMRXR	$K_2S_2O_7(l) \rightarrow K_2SO_4(l) + SO_3(g)$	(1.8)
R-4	HITEMRXR	$SO_3(g) \rightarrow SO_2(g) + 0.5 O_2(g)$	(1.9)

Figure 1.2: Simplified schematic of the SA process. Includes reaction occurring in each unit along with reference to the Aspen Plus® model name in Figure 1.3 and the equation number in Chapter 1.

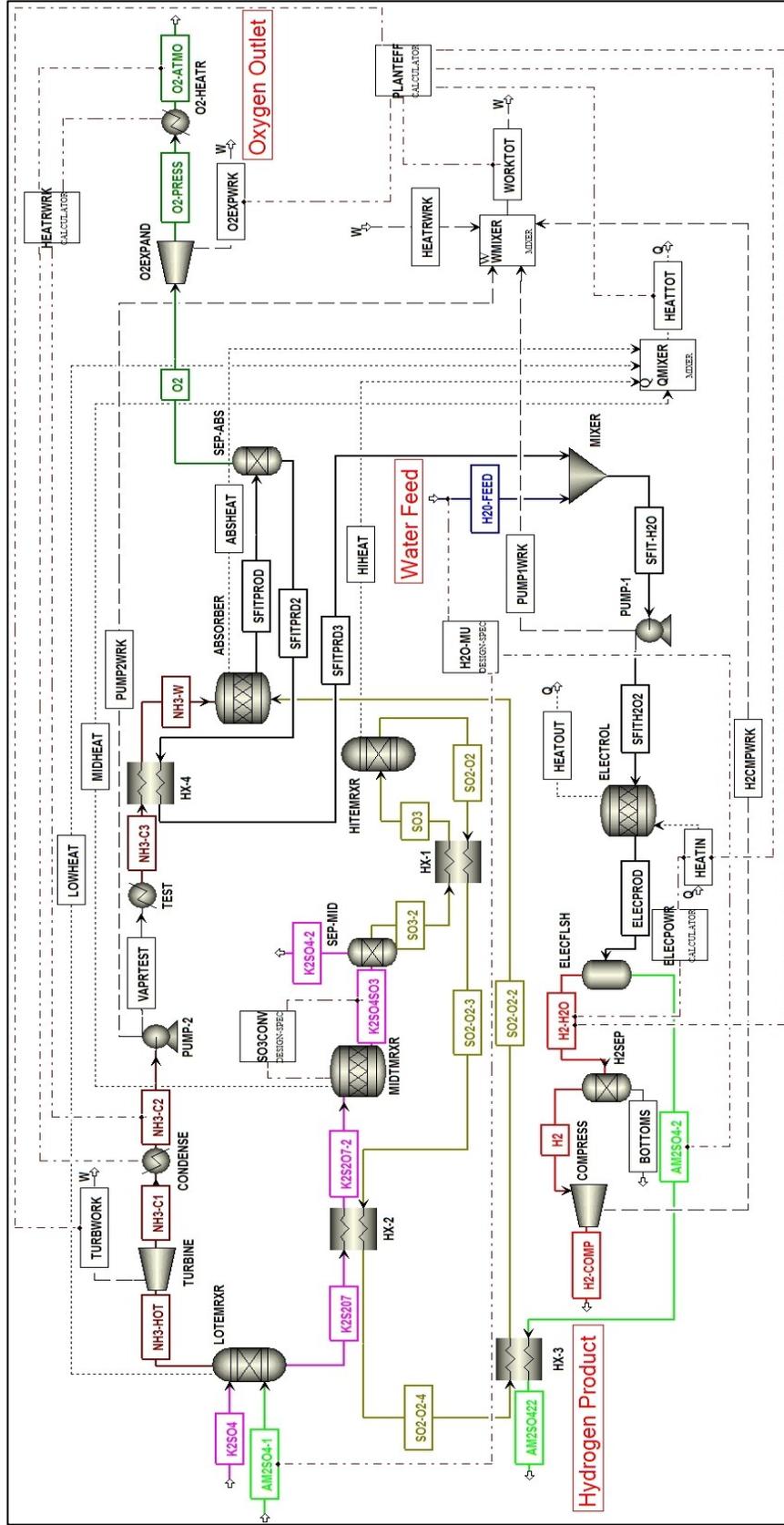


Figure 1.3: Flow sheet of the sulfur-ammonia solar thermochemical hydrogen production plant described in the current work.

Footnotes

¹ Aspen Plus is a registered trademark of Aspen Technology, Inc.

References

- [1] Akella, A., R. Saini, and M. Sharma., "Social, Economical and Environmental Impacts of Renewable Energy Systems," *Renewable Energy*, v.34, **2009**, p. 390-396
- [2] Ramachandran, R., Menon, R.K., "An Overview of Industrial Uses of Hydrogen," *International Journal of Hydrogen Energy*, v.23 **1998**, p. 593-598
- [3] Neef, H.-J., "International Overview of Hydrogen and Fuel Cell Research." *Energy*, v.34, **2009**, p. 327-333
- [4] Myers, D.B., Ariff, G.D., Kuhn, R.C., James, B.D., "Hydrogen from Renewable Energy Sources: Pathways to 10 Quads for Transportation Uses in 2030 to 2050," *Hydrogen, Fuel Cells, and Infrastructure Technologies*, FY **2003** Progress Report
- [5] Taylor, R., Davenport, R., T-Rassi, A., Muradove, N., Huang, C., Fenton, S., Genders, D., Symons, P., "Solar High-Temperature Water-Splitting Cycle with Quantum Boost," *DOE Hydrogen Program: FY 2010 Annual Progress Report*, **2010**, p. 120-125
- [6] Baykara, S., "Experimental Solar Water Thermolysis," *International Journal of Hydrogen Energy*, v.29 **2004**, p. 1459-1469
- [7] Funk, J.E., "Thermochemical Hydrogen Production: Past and Present," *International Journal of Hydrogen Energy*, v.26, **2001**, p. 185-190
- [8] Abanades, S., Charvin, P., Flamant, G., Neveu, P., "Screening of Water-Splitting Thermochemical Cycles Potentially Attractive for Hydrogen Production by Concentrated Solar Energy," *Energy*, v.31, **2006**, p. 2805-2822
- [9] Steinfeld, A., "Solar Hydrogen Production via a Two-Step Water-Splitting Thermochemical Cycle based on Zn/ZnO Redox Reactions," *International Journal of Hydrogen Energy*, v.27, **2002**, p. 611-619
- [10] Perkins, C., Weimer, A.W., "Likely Near-Term Solar-Thermal Water Splitting Technologies," *International Journal of Hydrogen Energy*, v.29, **2004**, p. 1587-1599

- [11] O'Keefe, D., Allen C., Besenbruch, G., Brown, L., Norman, J., Sharp, R., McCorkle, K., "Preliminary Results from Bench-Scale Testing of a Sulfur-Iodine Thermochemical Water-Splitting Cycle," *International Journal of Hydrogen Energy*, v.7, **1982**, p. 381-392
- [12] T-Raissi, A., Muradove, N., Huang, C., Adebiyi, O., "Hydrogen from Solar via Light-Assisted High-Temperature Water Splitting Cycles," *Journal of Solar Energy Engineering*, v.129, **2007**, p. 184-189
- [13] "DOE H2A Analysis." *DOE Hydrogen and Fuel Cells Program*. N.p., n.d. Web. 15 Aug. 2012. <http://www.hydrogen.energy.gov/h2a_analysis.html>.
- [14] "Florida Solar Energy Center." *Florida Solar Energy Center*. N.p., n.d. Web. 15 Aug. 2012. <<http://www.fsec.ucf.edu/en/>>.

Chapter 2: Aspen Plus® Model Chemistry

2.1 General Chemistry

The thermochemical SA process for hydrogen production consists of a set of chemical reactions that include the thermal decomposition of molten potassium pyrosulfate and gaseous sulfur trioxide in the oxygen production half-cycle and the electrolytic oxidation of aqueous ammonium sulfate in the hydrogen production half-cycle. These reactions were defined in Aspen Plus® by using the Chemistry section of the data browser (refer to Figure 2.1 for the location within the data browser). The chemistry for the chemical absorber (Eq. 1.10) was labeled ABSRXNS and is shown in Figure 2.2. Reaction 2 was placed in the set to account for any excess SO₃ and NH₃ that may enter or be present in the absorber. The chemistry for the electrolyzer was labeled ELECRXN (Eq. 1.11) and is shown in Figure 2.3. Because of the possibility of the formation of sulfuric acid, H₂SO₄ was placed in the chemistry subset to define the equilibrium of water with sulfur trioxide (refer to Figure 2.4). The chemistry for the high temperature reactor was labeled HIGHRXN (Eq. 1.9) and is shown in Figure 2.5. The chemistry for the low temperature reactor was labeled LOWRXNS (Eq. 1.7) and is shown in Figure 2.6. Reaction 2 was placed in the set for the remaining ammonium sulfite from the electrolyzer and its possible decomposition. The chemistry for the mid-temperature reactor was labeled MIDRXN (Eq. 1.8) and is shown in Figure 2.7.

Figure 2.8 shows an example of how this chemistry was called to the individual blocks where the reactions are pertinent. The example shows the Block

Options in the data browser and where LOWRXNS was defined as the Chemistry ID.

Similar methods were used throughout the flow sheet.

The ELECHEMA subset is defined in Section 2.2.

2.2 Electrolyte Chemistry

Electrolytes were an important aspect of this work. Potassium and ammonium salts are present as a liquid or as an aqueous solution. To define the electrolyte chemistry, the Electrolyte Wizard was used to determine the various possible electrolyte reactions that occur in the process. The location of the Electrolyte Wizard is shown in Figure 2.9. Once the Electrolyte Wizard in Aspen Plus[®] was completed, it generated the electrolyte reactions (defined as ELECHEMA in the Chemistry subsection of the data browser) and placed the additional ionic components shown in Figure 2.9. The reactions in ELECHEMA are defined in Table 2.1.

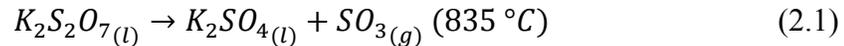
Table 2.1: Stoichiometric results of the Electrolyte Wizard.

Reaction	Type	Stoichiometry	Equation
1	Equilibrium	$\text{H}_2\text{O} + \text{HSO}_3^- \rightleftharpoons \text{H}_3\text{O}^+ + \text{SO}_3^{2-}$	(2.1)
2	Equilibrium	$2 \text{H}_2\text{O} + \text{SO}_2 \rightleftharpoons \text{H}_3\text{O}^+ + \text{HSO}_3^-$	(2.2)
3	Equilibrium	$\text{H}_2\text{O} + \text{H}_2\text{SO}_4 \rightleftharpoons \text{H}_3\text{O}^+ + \text{HSO}_4^-$	(2.3)
4	Equilibrium	$\text{H}_2\text{O} + \text{HSO}_4^- \rightleftharpoons \text{H}_3\text{O}^+ + \text{SO}_4^{2-}$	(2.4)
5	Equilibrium	$\text{H}_2\text{O} + \text{NH}_3 \rightleftharpoons \text{OH}^- + \text{NH}_4^+$	(2.5)
6	Equilibrium	$2 \text{H}_2\text{O} \rightleftharpoons \text{OH}^- + \text{H}_3\text{O}^+$	(2.6)
K2SO4	Dissociation	$\text{K}_2\text{SO}_4 \rightarrow \text{SO}_4^{2-} + 2 \text{K}^+$	(2.7)
AM2SO3	Dissociation	$\text{AM}_2\text{SO}_3 \rightarrow \text{SO}_3^{2-} + 2 \text{NH}_4^+$	(2.8)
AM2SO4	Dissociation	$\text{AM}_2\text{SO}_4 \rightarrow \text{SO}_4^{2-} + 2 \text{NH}_4^+$	(2.9)

This subset of electrolyte reactions was used as the global chemistry for the flow sheet except where otherwise noted.

2.3 Thermodynamics of Molten Salts

The oxygen production half-cycle of the current work involves high temperature liquid potassium sulfate and potassium pyrosulfate salts. This leads to the decomposition of potassium pyrosulfate to potassium sulfate and sulfur trioxide according to Eq. 2.1.



The decomposition of SO_3 to SO_2 and O_2 completes the oxygen half-cycle.

Simulation of these molten salts proved to be difficult. Aspen Plus[®] did not have any thermodynamic data regarding the potassium or ammonium salts in their solid or liquid state. To design an accurate flow sheet of the process, thermodynamic data from [1] was used. In particular, $\Delta H^\circ_{298.15 \text{ K}}$ [J/mol], $S^\circ_{298.15 \text{ K}}$ [J/mol·K], and C_p [J/mol·K] were used for the design of the flow sheet. Table 2.2 shows the values used for the previously mentioned parameters.

Table 2.2: Thermodynamic parameters $\Delta H^\circ_{298.15 \text{ K}}$ [J/mol] and $S^\circ_{298.15 \text{ K}}$ [J/mol·K] for K_2SO_4 and $K_2S_2O_7$ [1].

Component	Temperature range [K]	$\Delta H^\circ_{298.15 \text{ K}}$ [J/mol]	$S^\circ_{298.15 \text{ K}}$ [J/mol·K]
K_2SO_4	298.15 to 800	-1393665.4	211.5102
$K_2S_2O_7$	298.15 to 3000	-1971380.1	285.7865

A phase diagram of the $K_2SO_4 + K_2S_2O_7$ system was included in [1]. This diagram is shown in Figure 2.10. The phase diagram shows equilibrium data for the different phases of the $K_2SO_4 + K_2S_2O_7$ system. For the current work, the region of interest was the set of points between approximately 850 K and 1050 K and a composition of 0% to 30% K_2SO_4 . This region shows equilibrium between the liquid salts and liquid salts with gaseous SO_3 at a pressure of 0.1 MPa. These data were used

to accurately simulate the equilibrium between the liquid salts and the gaseous SO_3 .

Section 3.2.4 shows how these data were used in a design specification block and

Section 5.6 shows the results of this block.

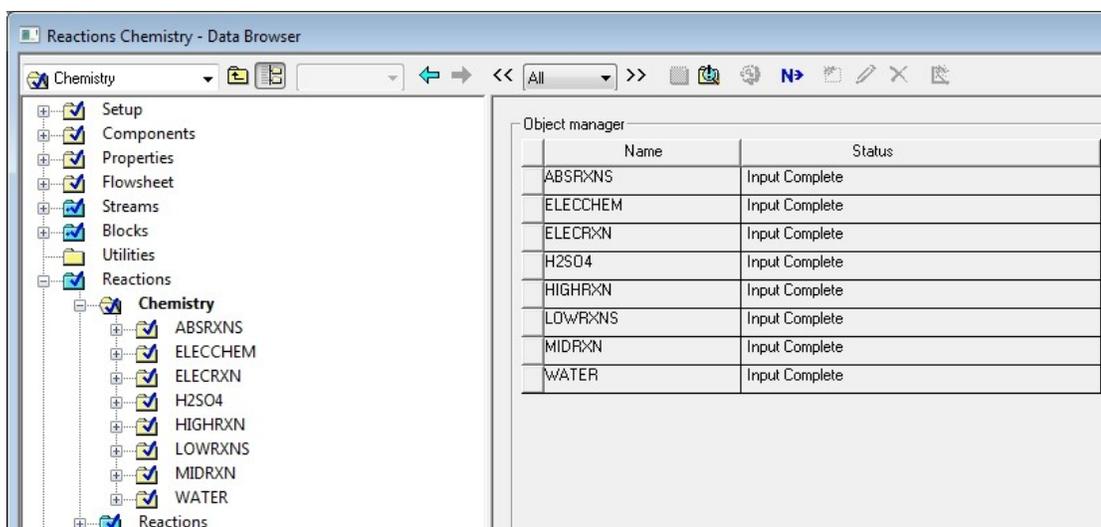


Figure 2.1: Location of the Chemistry sub-menu in the data browser. Each set of reactions used in the flow sheet is listed here.

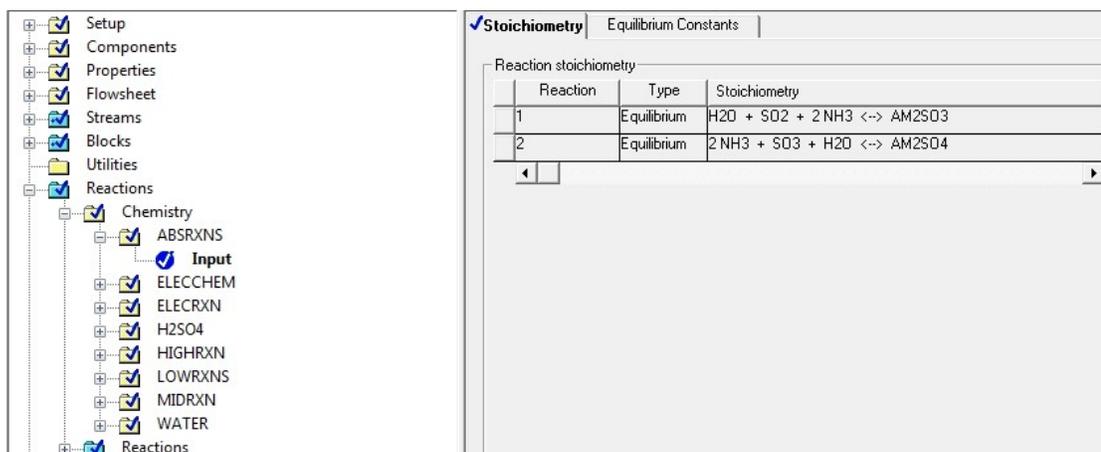


Figure 2.2: Location and definition of the reactions which occurred in the chemical absorber as defined in the flow sheet.

The screenshot shows a software interface with a tree view on the left and a 'Stoichiometry' tab on the right. The tree view includes 'Setup', 'Components', 'Properties', 'Flowsheet', 'Streams', 'Blocks', 'Utilities', and 'Reactions'. Under 'Reactions', there is a 'Chemistry' folder containing 'ABSRXNS', 'ELECCEM', 'ELEC RXN', 'Input', 'H2SO4', 'HIGH RXN', 'LOW RXNS', 'MID RXN', and 'WATER'. The 'Input' reaction is selected. The 'Stoichiometry' tab shows a table with the following data:

Reaction	Type	Stoichiometry
1	Equilibrium	$\text{H}_2\text{O} + \text{AM}_2\text{SO}_3 \leftrightarrow \text{AM}_2\text{SO}_4 + \text{H}_2$

Figure 2.3: Location and definition of the reactions which occurred in the electrolyzer as defined in the flow sheet.

The screenshot shows a software interface with a tree view on the left and a 'Stoichiometry' tab on the right. The tree view is identical to Figure 2.3, with 'Input' selected. The 'Stoichiometry' tab shows a table with the following data:

Reaction	Type	Stoichiometry
1	Equilibrium	$\text{H}_2\text{SO}_4 \leftrightarrow \text{SO}_3 + \text{H}_2\text{O}$

Figure 2.4: Location and definition of the reactions associated with the formation of sulfuric acid.

The screenshot shows a software interface with a tree view on the left and a 'Stoichiometry' tab on the right. The tree view is identical to Figure 2.3, with 'Input' selected. The 'Stoichiometry' tab shows a table with the following data:

Reaction	Type	Stoichiometry
1	Equilibrium	$\text{SO}_3 \leftrightarrow \text{SO}_2 + 0.5 \text{O}_2$

Figure 2.5: Location and definition of the reactions which occurred in the high temperature reactor as defined in the flow sheet.

The screenshot shows a software interface with a tree view on the left and a 'Stoichiometry' tab on the right. The tree view includes folders for Setup, Components, Properties, Flowsheet, Streams, Blocks, Utilities, and Reactions. Under Reactions, there is a 'Chemistry' folder containing sub-folders for ABRXNS, ELECCHEM, ELECRXN, H2SO4, HIGHRXN, LOWRXNS, Input (selected), MIDRXN, WATER, and Reactions. The 'Stoichiometry' tab is active, showing a table with two rows of reaction definitions.

Reaction	Type	Stoichiometry
1	Equilibrium	$\text{AM2SD4} + \text{K2SO4} \leftrightarrow \text{H2O} + 2 \text{NH3} + \text{K2S2O7}$
2	Equilibrium	$\text{AM2SO3} \leftrightarrow \text{SO2} + \text{H2O} + 2 \text{NH3}$

Figure 2.6: Location and definition of the reactions which occurred in the low temperature reactor as defined in the flow sheet.

The screenshot shows a software interface with a tree view on the left and a 'Stoichiometry' tab on the right. The tree view is identical to Figure 2.6, with the 'Input' reaction selected. The 'Stoichiometry' tab is active, showing a table with one row of reaction definition.

Reaction	Type	Stoichiometry
1	Equilibrium	$\text{K2S2O7} \leftrightarrow \text{K2SO4} + \text{SO3}$

Figure 2.7: Location and definition of the reactions which occurred in the mid-temperature reactor as defined in the flow sheet.

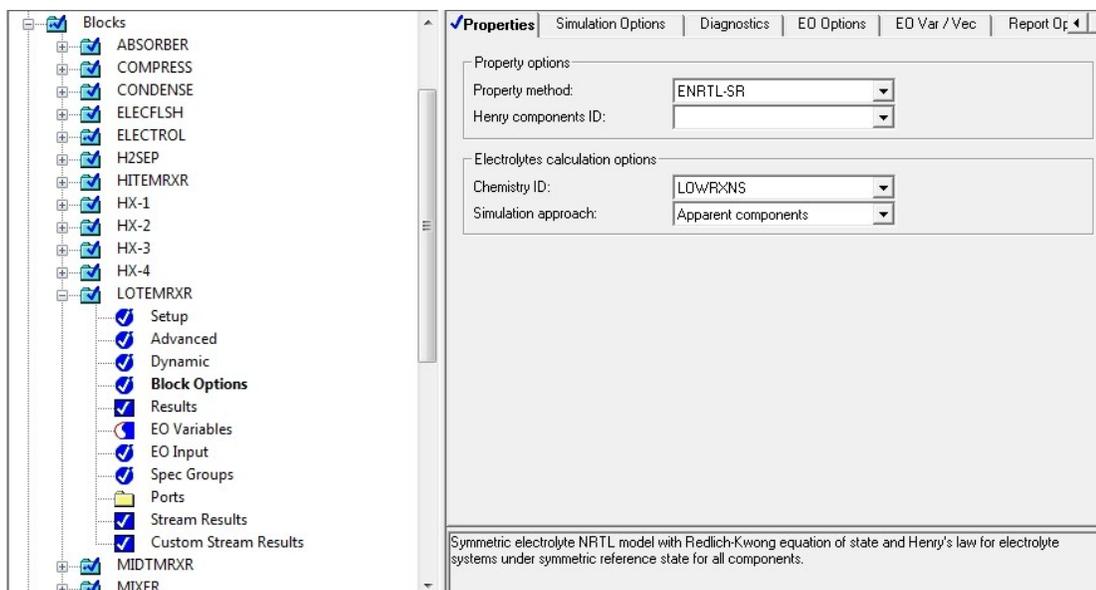


Figure 2.8: Example of how the chemistry was defined in the low temperature reactor.

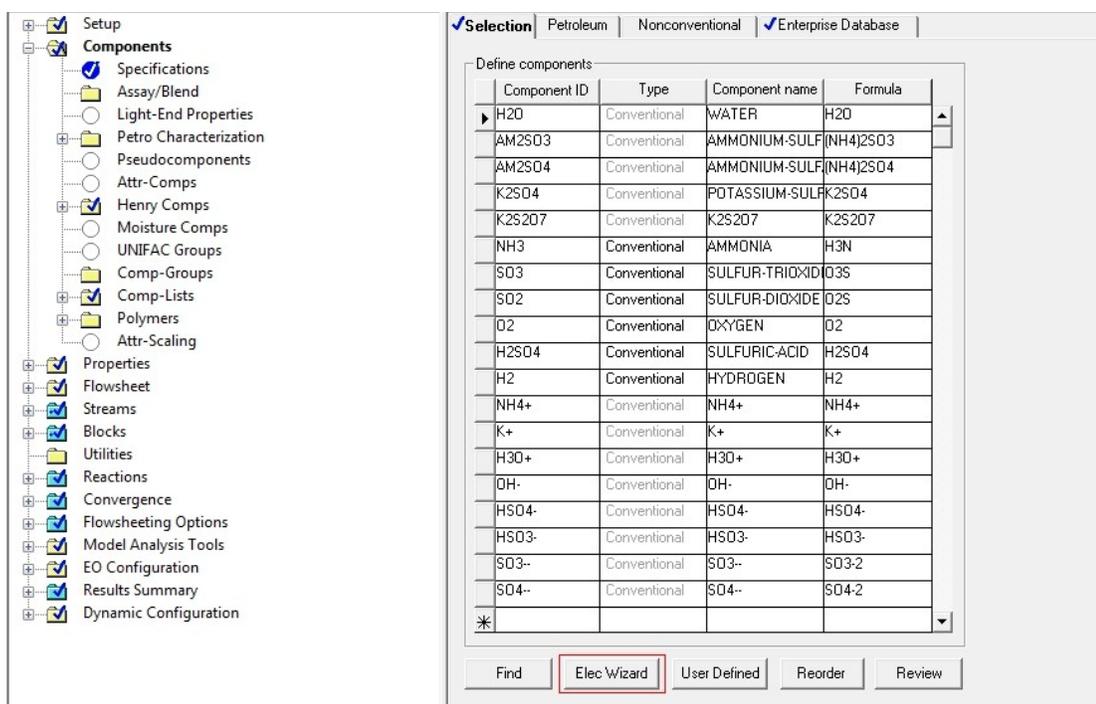


Figure 2.9: A list of the components necessary for this process including the components added by the Electrolyte Wizard which is accessed by the button at the bottom of this figure highlighted with a red box.

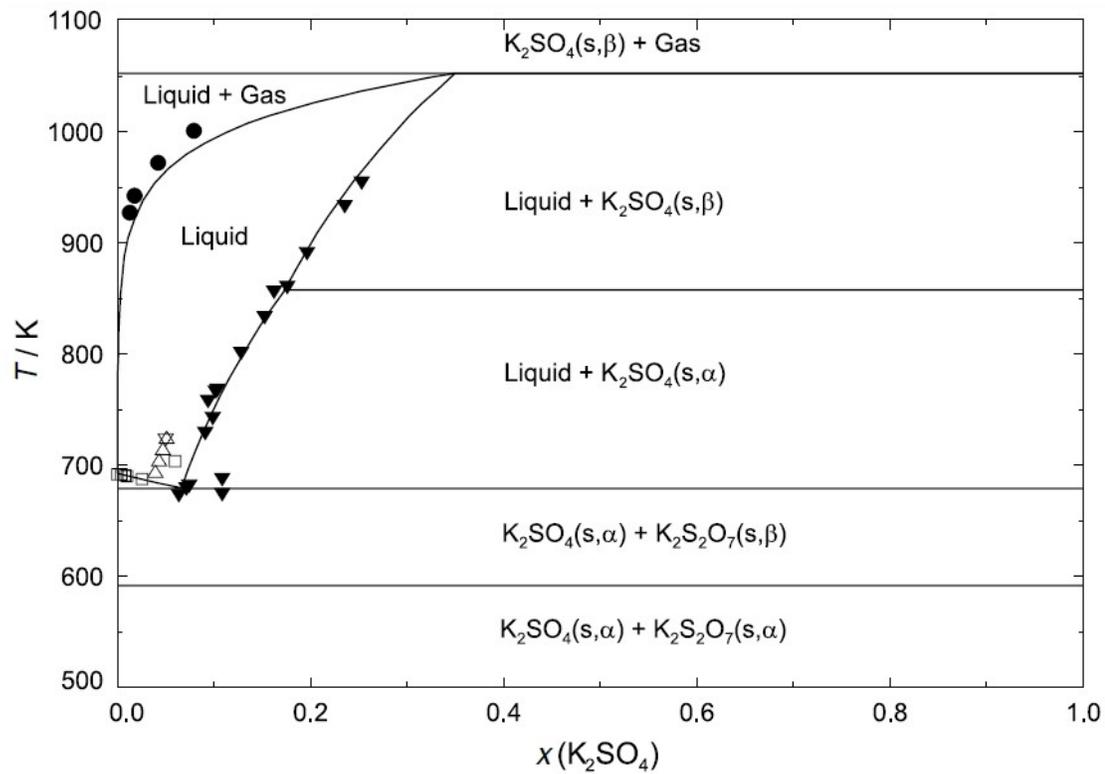


Figure 2.10: Phase diagram of the $\text{K}_2\text{SO}_4 + \text{K}_2\text{S}_2\text{O}_7$ system at a total pressure of 0.1 MPa [1].

References

- [1] Lindberg, D., Backman, R., Chartrand, P., "Thermodynamic Evaluation and Optimization of the (Na₂SO₄ + K₂SO₄ + Na₂S₂O₇ + K₂S₂O₇) System," *Journal of Chemical Thermodynamics*, v.38, **2006**, p. 1568-1583

Chapter 3: Aspen Plus® Model Methods

3.1 Simulations and Flow Sheet Design with Aspen Plus®

Aspen Plus® was used to simulate the SA solar thermochemical hydrogen (STCH) production plant in this work. Aspen Plus® V7.2 (24.0.4819) was the version used in this simulation. Aspen Plus® is a modeling environment for conceptual design, optimization, and performance monitoring for various industries including the chemical industry [1]. Aspen Plus® is used through a graphical user interface. There is minimal programming needed which is confined to the calculator and design specification blocks. Aspen Plus® uses thermodynamic models that govern the equilibrium relations for the simulated reactors and these thermodynamic models are incorporated within the program. Aspen Plus® was used to simulate the steady-state process to determine the feasibility and the efficiency of the process and incorporate laboratory data into the flow sheet.

3.2 Tools in Aspen Plus® and Their Use in the Flow Sheet

There are numerous tools within Aspen Plus® but only a few were used in this work. The process requires simulated reactors (names of the blocks, as seen in the model library, are noted in parentheses) including Gibbs (RGibbs) and stoichiometric (RStoich) reactors. The flow sheet includes many material, heat, and information flows. To achieve a more robust flow sheet, design specifications, calculator blocks, and sensitivity analyses were used throughout. Finally, after a pinch analysis, heat integration was performed using heat exchanger blocks (MHeatX). Miscellaneous

blocks will be described individually where pertinent but the main blocks used in the flow sheet are described below.

3.2.1 Thermodynamic Model ENRTL-SR and Property Input

The thermodynamic model chosen to govern the equilibrium relations within the reactors was the Electrolyte Non-Random Two-Liquid method that uses a symmetric reference state for ionic species (ENRTL-SR). This model calculates activity coefficients based on a symmetric reference state for ionic components of pure fused salts.

The symmetric option for the reference state for the activity coefficients of ionic components has to be chosen when using this method. This is necessary to ensure consistency across the simulation because this basis affects the equilibrium constants of electrolyte chemistry. It is not possible to combine symmetric and unsymmetric reference states for ions in the same simulation.

ENRTL-SR uses the symmetric electrolyte NRTL model GMENRTLS for the liquid phases with the symmetric reference state for ionic components and Henry's law for supercritical components. It uses the Redlich-Kwong equation of state for vapor phase.

To find this and more information on these property methods, the Aspen Plus[®] help menu can be used by searching “ENRTL-SR.”

The property databanks in Aspen Plus[®] did not contain all parameter values associated with the components needed for this process. In particular, the Gibbs energy ($\Delta G_{298.15}^{\circ}$ J/mol) and enthalpy ($\Delta H_{298.15}^{\circ}$ J/mol·K) of formation for $(\text{NH}_4)_2\text{SO}_3$,

$(\text{NH}_4)_2\text{SO}_4$, K_2SO_4 , and $\text{K}_2\text{S}_2\text{O}_7$ were input manually into the simulation in the properties section of the data browser. The enthalpy and entropy values were obtained from [2]. With the enthalpy and entropy, Eq. 3.1 was used to find the Gibbs energy change at the system temperature.

$$\Delta H = \Delta G - T\Delta S \quad (3.1)$$

Temperature ranges were given in [2] and meet the ranges required in this process. Refer to Figure 3.1 for the location in the data browser to input values and the parameter values entered.

3.2.2 The Gibbs reactor and the Low and High Temperature Reactors

The Gibbs reactor is an equilibrium reactor that performs chemical and phase equilibrium calculations by Gibbs energy minimization. For this information and more on Gibbs reactors in Aspen Plus[®], use help and search “gibbs reactor.” The reactor was chosen for the reactions simulated by the low and high temperature reactors because of the chemical and phase equilibrium calculations RGibbs is able to perform that are necessary in these two instances. RGibbs requires input of two of the following operating conditions: pressure, temperature, or heat duty. The user can also define the maximum number of fluid phases. RGibbs allows products to be defined to appear in certain phases.

The low temperature reactor was used to simulate the production of potassium pyrosulfate and ammonia described in Eq. 1.7. The low temperature reactor was labeled LOTEMRXX. The location of the low temperature reactor and all other blocks and streams referred henceforth can be seen in Figure 1.3. RGibbs was chosen

to simulate this reactor because it is capable of calculating phase equilibrium for the vapor-liquid system between liquid K_2SO_4 and $K_2S_2O_7$ and gaseous water and NH_3 .

Also, RGibbs was chosen because the kinetics involved in Eq. 1.7 was not known.

Figure 3.2 shows how the products were defined to appear in either the liquid or vapor phase.

The high temperature reactor was used to simulate the decomposition of sulfur trioxide described in Eq. 1.9. The high temperature reactor was labeled HITEMRXXR (Figure 1.3). RGibbs was chosen to simulate this reactor because the reaction kinetics was not input into the flow sheet.

Results for the low and high temperature reactors are in Section 5.3.

3.2.3 The Stoichiometric Reactor and the Mid-Temperature Reactor, Chemical Absorber, and Electrolyzer

The RStoich block models a reactor with specified reaction extent or conversion. For this information and more on stoichiometric reactors in Aspen Plus[®], use help and search “stoichiometric reactor.” The reactor was chosen for the reactions simulated by the mid-temperature reactor, chemical absorber, and electrolyzer. This reactor block was used for the mid-temperature reactor because thermodynamic data was known but the conversion of potassium pyrosulfate needed to be calculated by a design specification, for the chemical absorber because it was preferable to achieve 100% conversion of the ammonia, and for the electrolyzer because laboratory data on the conversion within the reactor were available.

The mid-temperature reactor was used to simulate the decomposition of potassium pyrosulfate described in Eq. 1.8. The mid-temperature reactor was labeled MIDTMRXR (Figure 1.3). RStoich was chosen to simulate this reactor because phase equilibrium data between liquid $K_2S_2O_7$ and K_2SO_4 and gaseous SO_3 were known [2]. A phase diagram from [2] was digitized and the resulting equation fit to the data was related to the mid-temperature reactor via a design specification block, SO3CONV (see Section 3.2.4 for further description of SO3CONV).

Eq. 1.10 is carried out in a reactive absorption process simulated by an RStoich reactor block. The chemical absorber was labeled ABSORBER (Figure 1.3). RStoich was chosen to simulate this reactor because it was preferable to achieve 100% conversion of the incoming ammonia. This stoichiometric reactor was manually set to convert 100% of the NH_3 feed.

Eq. 1.11 is carried out in an electrolytic process simulated by an RStoich reactor block. The electrolyzer was labeled ELECTROL (Figure 1.3). RStoich was chosen to simulate this reactor because there was available data on the molar concentration of $(NH_4)_2SO_4$ in the product stream from our partners at Electrosynthesis Company, Inc. working specifically on the electrolytic portion of this process. This stoichiometric reactor was set to convert 95.0% of the $(NH_4)_2SO_3$ feed.

Results for the mid-temperature reactor and the chemical absorber are described in Section 5.3 and the electrolyzer in Section 5.7.

3.2.4 Design Specification Blocks

Certain parameter values may need to be controlled to follow, in a specified way, the value of another parameter elsewhere in the process. In Aspen Plus[®], to achieve this control, a design specification block can be used. Design specifications were used throughout the simulation to create a more robust simulation that can handle changes made to input parameters and still converge on a reasonable table of values that represent the overall process.

Design specification blocks are constructed by first defining the flow sheet variables associated with the required value. Next, the specification is defined by either a constant or a FORTRAN expression in terms of the flow sheet variables defined previously. In this work, only the latter was used. Along with the specification, a target value must be defined. This can either be a constant or another FORTRAN expression in terms of the variables defined. Only the former was used in this work. A tolerance between the specification and the target must also be set and this can, once again, be either a constant or a FORTRAN expression. Only the former was used in this work. Last, the manipulated parameter is defined. Along with this definition are the manipulated variable limits. It is at this point that the designer must set the upper and lower bounds and has the ability to enter a step size, although the step size is not necessary.

A design specification is similar to a controller: parameter values can be set by varying other parameters within the plant. The final values obtained by the design specification will overwrite the initial, specified value for that block or stream. In this work, two design specifications were used: H2O-MU and SO3CONV to correct the

feed water flow rate for any losses from the two exit streams and to determine the conversion within the mid-temperature reactor, to agree with digitized laboratory results from [2], at temperature and pressure, respectively.

The design specification block H2O-MU was used to determine the make-up feed water required due to losses from the two exit streams. This block used two variables imported from the flow sheet: the molar flow rate of water into the low temperature reactor WH2O1 [kmol/hr] and the molar flow rate of water out of the electrolyzer WH2O2 [kmol/hr]. Figure 3.3 shows the location of H2O-MU in the data browser and how the variables were defined.

The specification of this block was defined by the following FORTRAN expression using the values defined previously

$$\frac{WH2O1[\frac{kmol}{hr}]}{WH2O2[\frac{kmol}{hr}]} \quad (3.2)$$

The target value for Eq. 3.2 was set to 1. This would force the two flow rates to be equal. The tolerance was set to 0.0001. See Figure 3.4 for the specification portion of this block.

To achieve a target value of 1, the water feed flow rate was varied (stream H2O-FEED). The lower and upper manipulated variable limits were set to 5,000 kmol/hr and 10,000 kmol/hr, respectively. Figure 3.5 shows the varied portion of this block.

The design specification block SO3CONV was used to determine the conversion within the mid-temperature reactor using digitized laboratory results from [2]. This block used three variables imported from the flow sheet: the mole fraction of

K_2SO_4 $X_{K_2SO_4}$, temperature T [$^{\circ}C$], and pressure P [bar] of the mid-temperature reactor product stream. The conversion in the mid-temperature reactor (CONV) was also defined but only as a reference to the user. Figure 3.6 shows the location of SO3CONV in the data browser and how the variables were defined.

Figure 2.10 is a phase diagram of the ($K_2S_2O_7 + K_2SO_4$) system where the gas is SO_3 [2]. Equilibrium at the upper liquid-gas interface is defined by

$$K_{eq}[\text{bar}] = \frac{P[\text{bar}]X_{K_2SO_4}}{1-X_{K_2SO_4}} \quad (3.3)$$

The curve in the phase diagram was digitized and an equation fit to the data points. Because Eq. 3.3 and the equilibrium values from the paper should be equal, the specification of this block was defined by the following FORTRAN expression using previously defined values

$$\left\{ 10^{[-9.94 + 22.6\left(\frac{T[^{\circ}C] + 273.15}{1000}\right) - 13.53\left(\frac{T[^{\circ}C] + 273.15}{1000}\right)^{0.838}]} \right\} \times \left\{ \frac{1 - X_{K_2SO_4}}{P[\text{bar}] \times X_{K_2SO_4}} \right\} \quad (3.4)$$

Notice the inverse of Eq. 3.3 in Eq. 3.4. The target value for Eq. 3.4 was set to 1. The tolerance was set to 0.0001. See Figure 3.7 for the specification portion of this block.

At a set temperature and pressure and to achieve a target value of 1, the mole fraction of K_2SO_4 in the outlet stream of the mid-temperature reactor, and therefore the conversion of $K_2S_2O_7$ to SO_3 and K_2SO_4 within the reactor, must be varied. The lower and upper manipulated variable limits were set to 0.001 and 0.999, respectively. See Figure 3.8 for the varied portion of this block.

Refer to Section 5.6 for the results of the H₂O-MU and SO₃CONV design specifications.

3.2.5 Calculator Blocks

While building a flow sheet, the designer may come to a point where a value is needed that cannot be supplied by Aspen Plus[®] with its various built-in tools because of the unique processes that need to be simulated. To calculate this value, the flow sheet may include a calculator block.

Calculator blocks are designed by first defining pertinent variables associated with the required value and their information flow (either imported or exported). Next, a FORTRAN code is written to calculate the required value. And last, that value can be exported and used where needed in the flow sheet or it can be displayed as a stand-alone value for reference to the designer. In the present work, the calculated value was exported and used for reference.

In this work, two calculator blocks were needed within the flow sheet: ELECPOWR and PLANTEFF to calculate the heat duty required by the electrolyzer dependent on the amount of hydrogen produced and the overall efficiency of the process, respectively (Figure 1.3).

The calculator block ELECPOWR was used to calculate the heat duty required by the electrolyzer dependent on the amount of hydrogen produced. This block used one variable imported from the flow sheet: the flow of hydrogen produced FH2 [kmol/hr]. The block then exported the power required to produce said amount of hydrogen by the electrolyzer ELECPOWR [Watt]. See Figure 3.9 for the location of ELECPOWR in the data browser and how the variables were defined.

The FORTRAN code written for ELECPOWR is shown in Figure 3.10. The code was written on the basis of electrochemical relations. The derivation is shown in

Appendix A. The value of 0.8 V for the potential difference between electrodes in the electrolyzer was given by Electrosynthesis Company, Inc. With this potential, the power requirement of the electrolyzer block could be found for any production rate of hydrogen.

The power requirement for electrolysis was exported directly to the electrolyzer via the heat stream HEATIN. Excess heat from the electrolyzer was rejected by the heat stream HEATOUT. Physically, this would be the heat lost by the internal components of the electrolysis system.

The calculator block PLANTEFF was used to calculate the overall efficiency of the process. This block used four variables imported from throughout the flow sheet, including the heat duty required by the electrolyzer ELECPOWR [Watt], the work generated by the heat recovery system TURBWORK [Watt], the flow of hydrogen out of the process FH2 [kmol/hr], and the total heat required for the solar reactors HEATTOT [Watt]. See Figure 3.11 for the location of PLANTEFF in the data browser and the definition of the variables.

The FORTRAN code written for PLANTEFF is shown in Figure 3.12. The code was written on the basis of the definition of overall plant efficiency defined by the DOE. See Section 5.9 for more information on the definition of the efficiency. With this calculator block, the efficiency could be determined each time convergence was achieved and with any changes made within the flow sheet.

The efficiency block then exported two variables: LHV [Watt], the lower heating value of hydrogen as described in Appendix B, and ETA, the overall efficiency of the plant.

Results of the ELECPOWR and PLANTEFF calculator blocks are located in Section 5.7.

3.2.6 Sensitivity Analyses

While building the flow sheet, the designer may need to know the dependence of any number of parameters on one parameter in the process if any such relationship exists. To find this dependence, the flow sheet may include a sensitivity analysis.

Sensitivity analyses are designed by first defining pertinent variables associated with a dependent relationship that is to be determined. Next, the independent variable is defined with lower and upper limits. And last, the independent variable, along with any number of the dependent variables, is tabulated for ease of reference or plotting needs.

In this work, two sensitivity analyses were conducted within the flow sheet: NH3VAPOR and SO3PROD to determine, at constant pressure, the temperature just before the NH₃-water stream vaporized and the temperature at which the necessary amount of SO₃ was produced in the mid-temperature reactor, respectively.

The sensitivity analysis NH3VAPOR was used to determine, at constant pressure, the temperature that the condensed ammonia-water stream would vaporize. This was accomplished by placing a test heater block in the condensed stream. The temperature of the heater was varied and the vapor fraction of the outgoing stream (NH3-C3) was tabulated. This analysis used two variables imported from the flow sheet: the vapor fraction of the ammonia-water stream VAPRFAC and the temperature of the heater block T [°C]. The block then tabulated these two variables

for later reference. See Figure 3.13 for the location of NH3VAPOR in the data browser and the definitions of the variables.

The independent variable was now defined as the manipulated variable. The temperature of the heater block was varied as shown in Figure 3.14 and incremented by 1 °C. Last, the two variables were tabulated by pressing the “Fill variables” button in the lower right-hand portion of Figure 3.15.

The sensitivity analysis SO3PROD was used to determine, at constant pressure, the temperature of the mid-temperature reactor to produce a necessary amount of SO₃. This analysis used two variables imported from the flow sheet: the SO₃ product FSO3 [kmol/hr] and the temperature T [°C] of the mid-temperature reactor. The block then tabulated these two variables for later reference. See Figure 3.16 for the location of SO3PROD in the data browser and the definitions of the variables.

The independent variable was now defined as the manipulated variable. The temperature of the mid-temperature reactor was varied as shown in Figure 3.17 and incremented by 0.5 °C. Last, the two variables were tabulated by pressing the “Fill variables” button in the lower right-hand portion of Figure 3.18.

Results of the NH3VAPOR and SO3PROD sensitivity analyses are located in Section 5.8.

3.3 Pinch Analysis, Heat Integration, and the MHeatX Block

In the present work, a standard pinch analysis procedure was performed for heat integration. The procedure laid out, in detail, by Turton et al. was used as a reference to perform the heat integration [3].

For heat integration, the heat capacity C_p [J/kg·K] values for streams that would be used for transferring heat were required. To do this, RStoich reactors were placed in those streams and defined with one pertinent reaction and a zero conversion. This was done to prevent any changes to the stream or its properties through the reactor. Across the reactor, the temperature was changed by $0.1 \Delta T$ [K]. This method does not take into account the temperature dependence of heat capacity ($C_p(T)$). By doing this, the heat duty Q [Watt] of the reactor was calculated by Aspen Plus[®]. With the heat duty, the following equations were used to find the heat capacity

$$Q[W] = \dot{m} \left[\frac{kg}{s} \right] C_p \left[\frac{J}{kg \cdot K} \right] \Delta T [K] \text{ (where } \Delta T = 0.1 K \text{)} \quad (3.5)$$

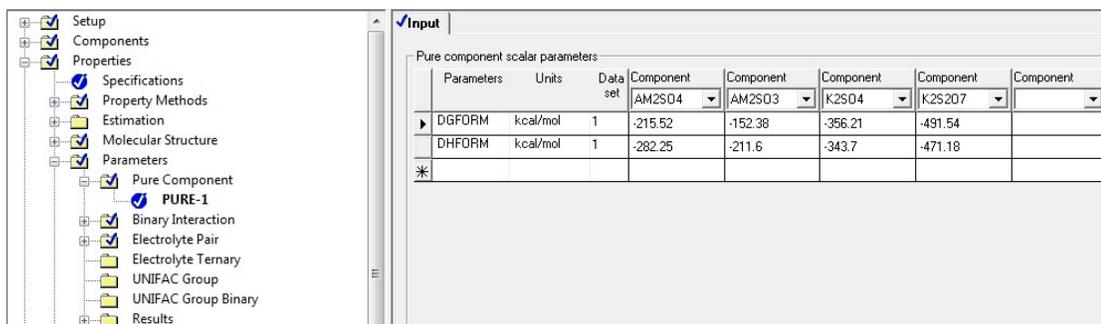
$$\Rightarrow C_p \left[\frac{J}{kg \cdot K} \right] = \frac{Q[W]}{\dot{m} \left[\frac{kg}{s} \right] \Delta T [K]} \quad (3.6)$$

In Eqs. 3.5 and 3.6, \dot{m} [kg/s] is the mass flow rate through the reactor. With the heat capacities, a standard pinch analysis was used to finish the heat integration.

To more accurately simulate the heat transfer between streams, heat exchangers were placed throughout the flow sheet to accommodate the transfer of heat. Specifically, MHeatX was chosen from the model library as the heat exchanger. MHeatX was chosen for its ability to be designed by the input of information obtained from the pinch analysis and simplicity of use. With a hot stream and cold stream, the designer has the ability to define only one temperature of either outlet. The heat

exchanger block then calculates the heat duty required while also alerting the user of temperature crossovers.

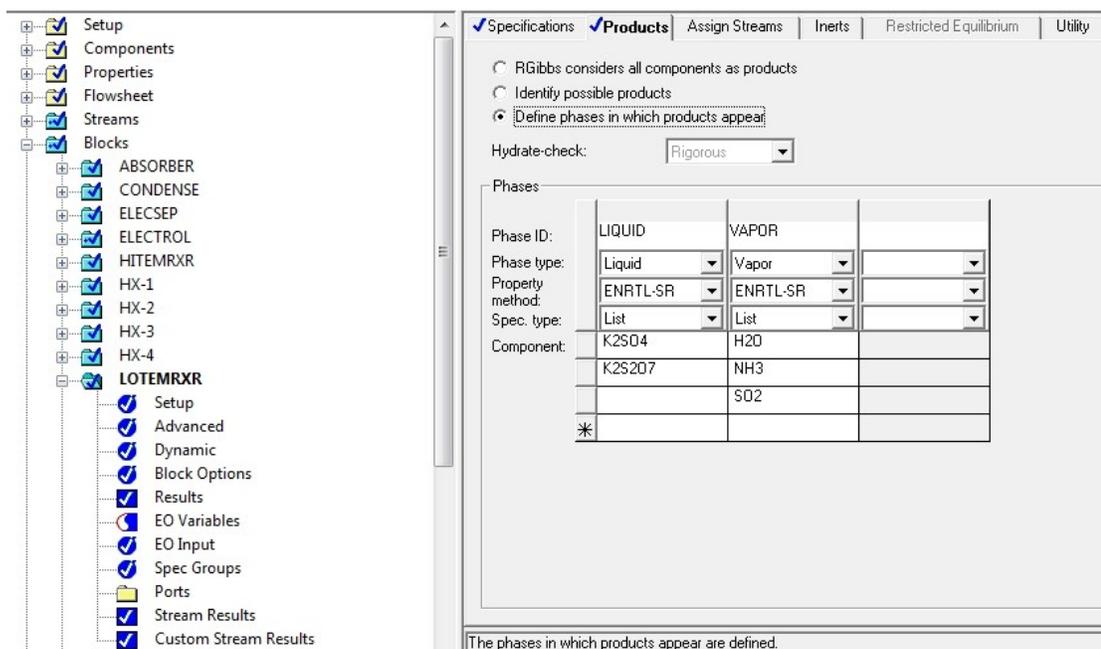
Refer to Chapter 5.4 for results obtained from the pinch analysis.



Pure component scalar parameters

Parameters	Units	Data set	Component	Component	Component	Component	Component
			AM2SD4	AM2SD3	K2S04	K2S2O7	
DGFORM	kcal/mol	1	-215.52	-152.38	-356.21	-491.54	
DHF0RM	kcal/mol	1	-282.25	-211.6	-343.7	-471.18	
*							

Figure 3.1: Location of properties for $(\text{NH}_4)_2\text{SO}_3$, $(\text{NH}_4)_2\text{SO}_4$, K_2SO_4 , and $\text{K}_2\text{S}_2\text{O}_7$ in data browser and the values of the Gibbs energy and enthalpy changes for the respective species.



Specifications Products Assign Streams Inerts Restricted Equilibrium Utility

RGibbs considers all components as products
 Identify possible products
 Define phases in which products appear

Hydrate-check: Rigorous

Phases

Phase ID:	LIQUID	VAPOR	
Phase type:	Liquid	Vapor	
Property method:	ENRTL-SR	ENRTL-SR	
Spec. type:	List	List	
Component:	K2S04	H2O	
	K2S2O7	NH3	
		SO2	
*			

The phases in which products appear are defined.

Figure 3.2: Defined phases of the products within the LOTEMRXR RGibbs reactor along with its location in the data browser.

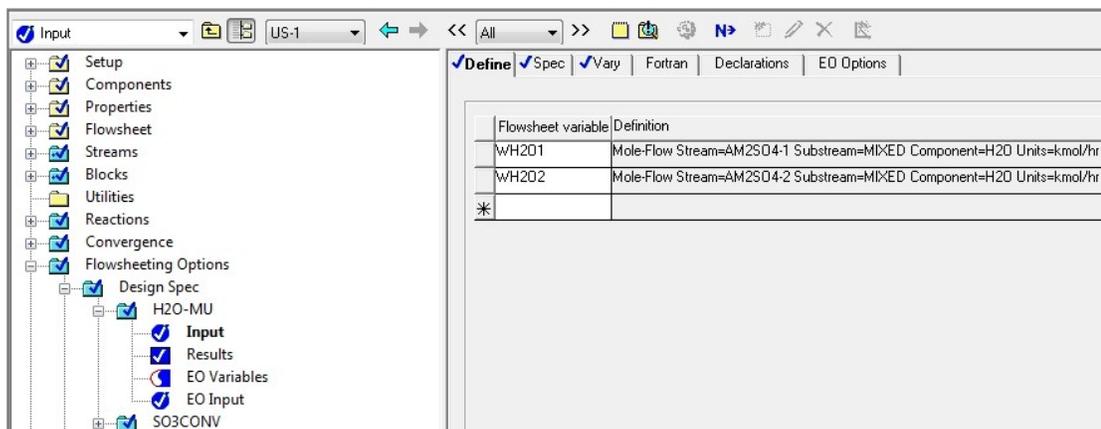


Figure 3.3: Location of H2O-MU in the data browser and the definitions of the variables used.

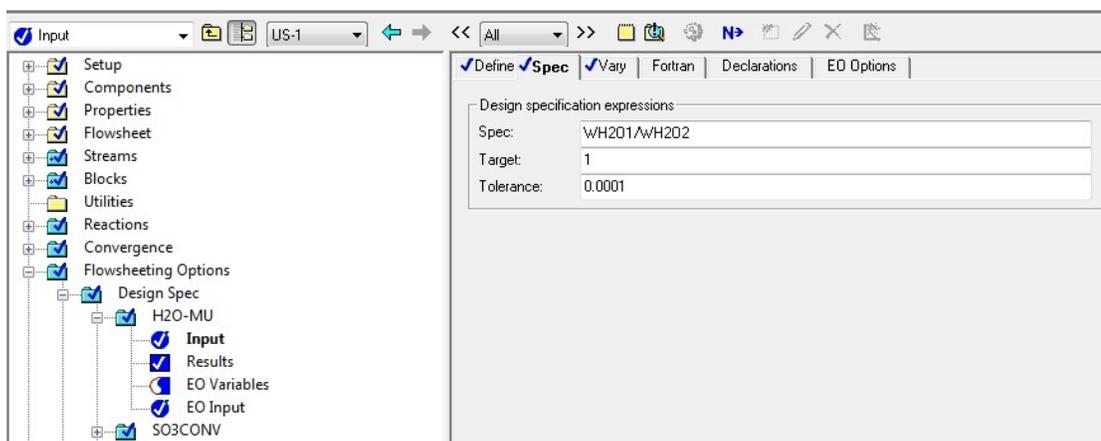


Figure 3.4: Shows specification, target, and tolerance for H2O-MU block.

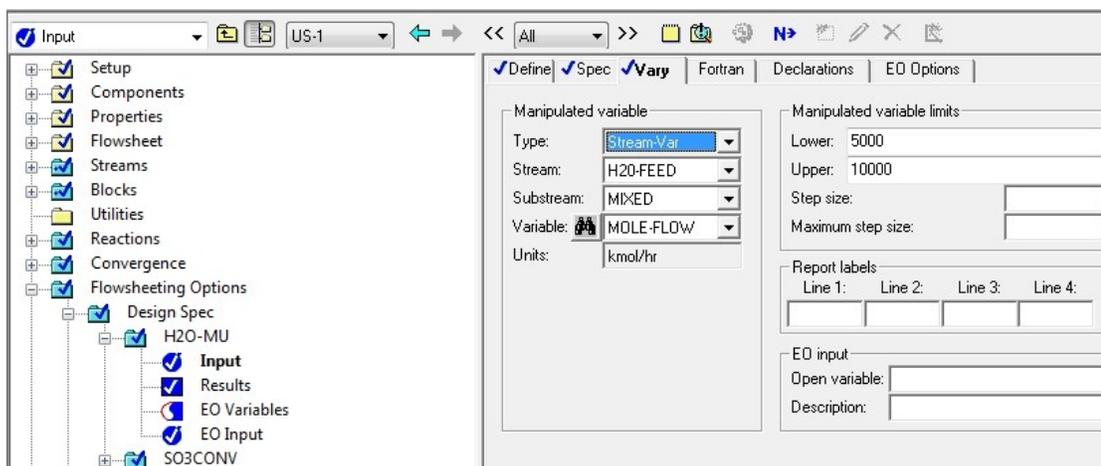


Figure 3.5: Shows the manipulated variable and its limits for H2O-MU block.

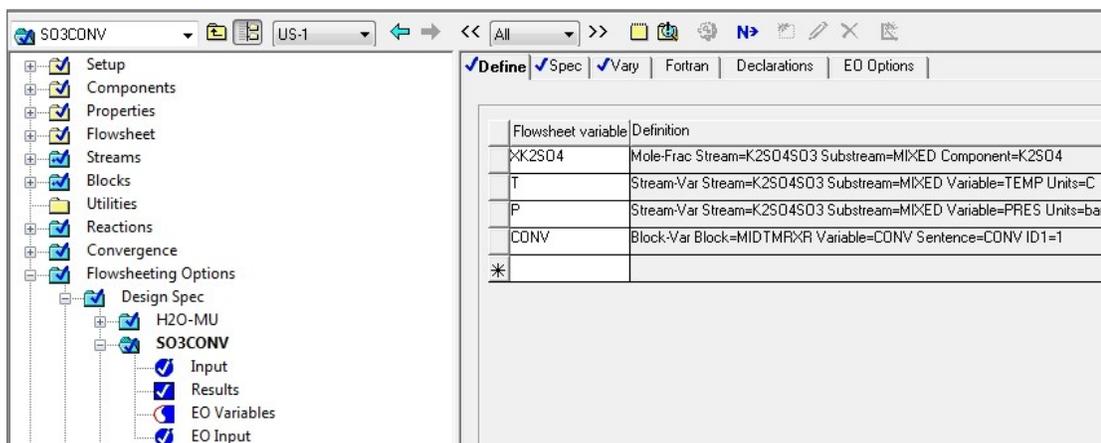


Figure 3.6: Location of SO3CONV in the data browser and the definitions of the variables used.

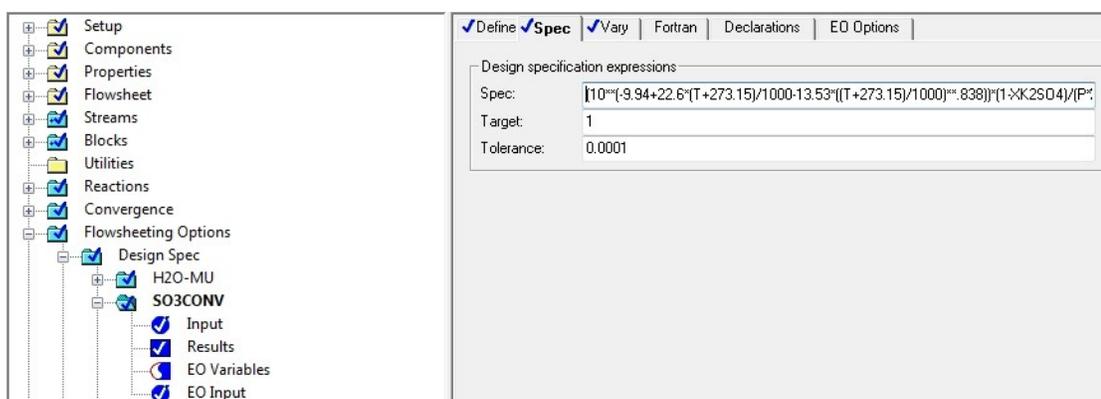


Figure 3.7: Shows specification, target, and tolerance for SO3CONV block.

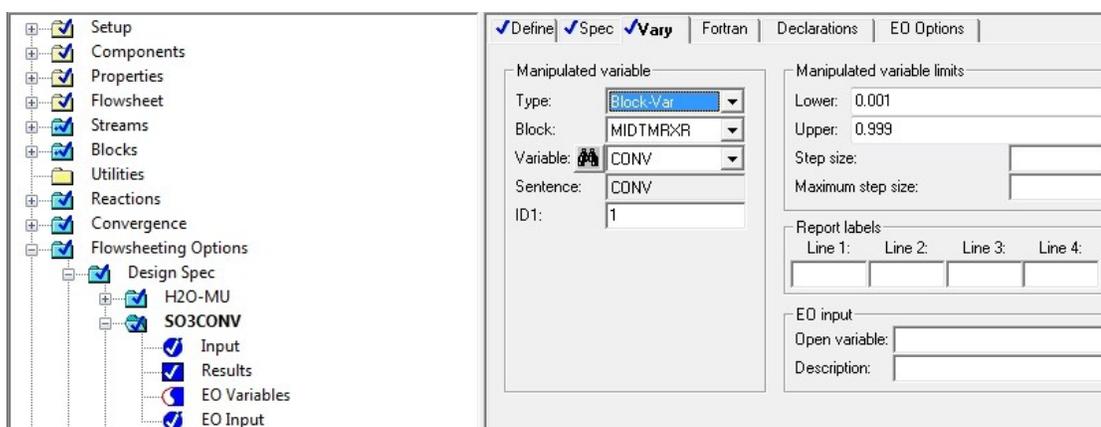


Figure 3.8: Shows the manipulated variable and its limits for SO3CONV block.

The screenshot shows the Aspen Plus data browser interface. On the left, a tree view displays the project hierarchy, with 'ELECPOWR' selected under the 'Calculator' block. On the right, the 'Define' tab is active, showing a table of variable definitions:

Variable name	Info. flow	Definition
FH2	Import	Mole-Flow Stream=H2 Substream=ML:ED Component=H2 Units=kmol/hr
ELECPOWR	Export	Heat-Duty Stream=HEATIN Units=Watt
*		

Figure 3.9: Shows the location of the ELECPOWR calculator in the data browser and the definitions of the variables used.

The screenshot shows the Aspen Plus data browser with the 'ELECPOWR' calculator selected. The 'Calculate' tab is active, displaying the FORTRAN code used for the calculation. The code is as follows:

```

C - Comments start with capital C in column 1
C - Executable statements start in column 7
C - This block calculates the power required for the electrolyzer
C - by importing the flow of H2 out of the block and using simple
C - electrodynamic equations
C - let F = Faraday's constant at 96,486 C/mol
C - let E = voltage V
  F = 96485
  E = 0.8
  ELECPOWR = (2 * 1000 * F * FH2 * E) / 3600
C - Factor of 1000 because FH2 is in terms of kmol/hr; need to
C - convert to mol/hr first:
C - then divide by 3600 because ultimately need Fh2 in terms of mol/s
C - Divide again by 1000 because equations worked out were in units of
C - Watts; Aspen decided on output units of kiloWatts so it was
C - necessary to convert units to match those in Aspen

```

Figure 3.10: Shows the FORTRAN code for ELECPOWR along with its location within the data browser.

The screenshot shows the data browser on the left with the following tree structure:

- Setup
- Components
- Properties
- Flowsheet
- Streams
- Blocks
- Utilities
- Reactions
- Convergence
- Flowsheeting Options
- Design Spec
- Calculator
 - ELECPWR
 - PLANTEFF**
 - Input
 - Block Options
 - Results
 - EO Variables
 - EO Input

The right pane shows the 'Define' tab with the following table:

Variable name	Info. flow	Definition
ELECPWR	Import	Heat-Duty Stream=HEATIN Units=Watt
TURBWORK	Import	Work-Power Stream=TURBWORK Units=Watt
FH2	Import	Mole-Flow Stream=H2 Substream=MIXED Component=H2 Units=kmol/hr
HEATTOT	Import	Heat-Duty Stream=HEATTOT Units=Watt
ETA		Local-Param Physical type=Dimensionless Units=Unitless
LHV		Local-Param Physical type=Power Units=Watt
*		

Figure 3.11: Shows the location of the PLANTEFF calculator in the data browser and the definitions of the variables used.

The screenshot shows the data browser on the left with the following tree structure:

- Setup
- Components
- Properties
- Flowsheet
- Streams
- Blocks
- Utilities
- Reactions
- Convergence
- Flowsheeting Options
- Design Spec
- Calculator
 - ELECPWR
 - PLANTEFF
 - Input**
 - Block Options
 - Results
 - EO Variables
 - EO Input
- Transfer
- Stream Library
- Balance
- Measurement
- Pres Relief
- Add Input

The right pane shows the 'Calculate' tab with the following FORTRAN code:

```

Calculation method
 Fortran  Excel 

Enter executable Fortran statements
C - Comments start with capital C in column 1
C - Executable statements start in column 7
C - This block calculates the efficiency of the entire plant by
C - importing the flow of H2 out of the electrolyzer, the electrical
C - power required by the electrolyzer calculated by the calculator
C - block ELECPWR, the work out of the turbine, and the total heat
C - required by the 3 reactors and the absorber summed together by the
C - HEATTOT block. The efficiency is calculated using the DOE definition
C - of ETA = LHV H2 / ((ELECTROL POWER-TURBINE WORK OUT) + TOTAL HEAT) .
C - Let LHV be the lower heating value of H2
      LHV = 67177.6 * FH2
      ETA = LHV / ((ELECPWR + TURBWORK) - HEATTOT)
C - To calculate the LHV of H2, a conversion factor of 119.955 was
C - obtained from the DOE website (that calculates the LHV of H2 at
C - different quantities) .
  
```

Figure 3.12: Shows the FORTRAN code for PLANTEFF along with its location within the data browser.

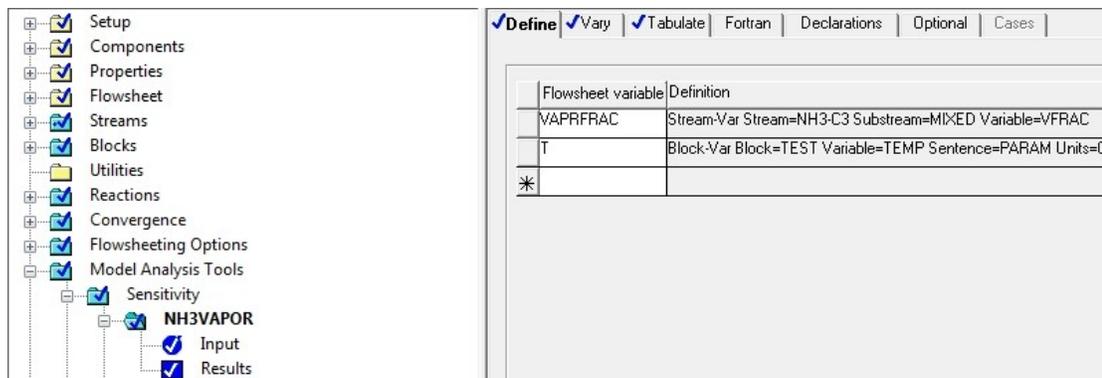


Figure 3.13: Shows the location of the sensitivity block NH3VAPOR and the definitions of the variables used.

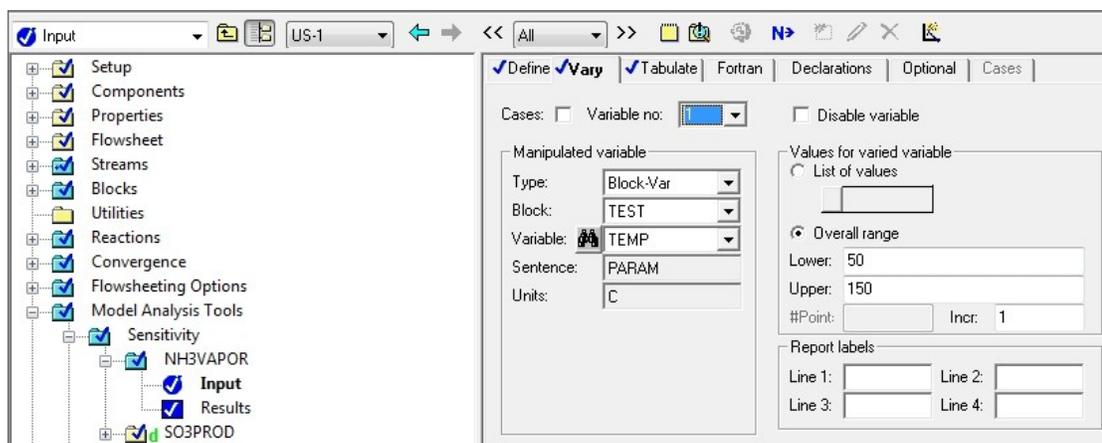


Figure 3.14: The temperature of the test heater block was defined as the manipulated variable in NH3VAPOR, ranged from 50 to 150 °C, and incremented by 1 °C.

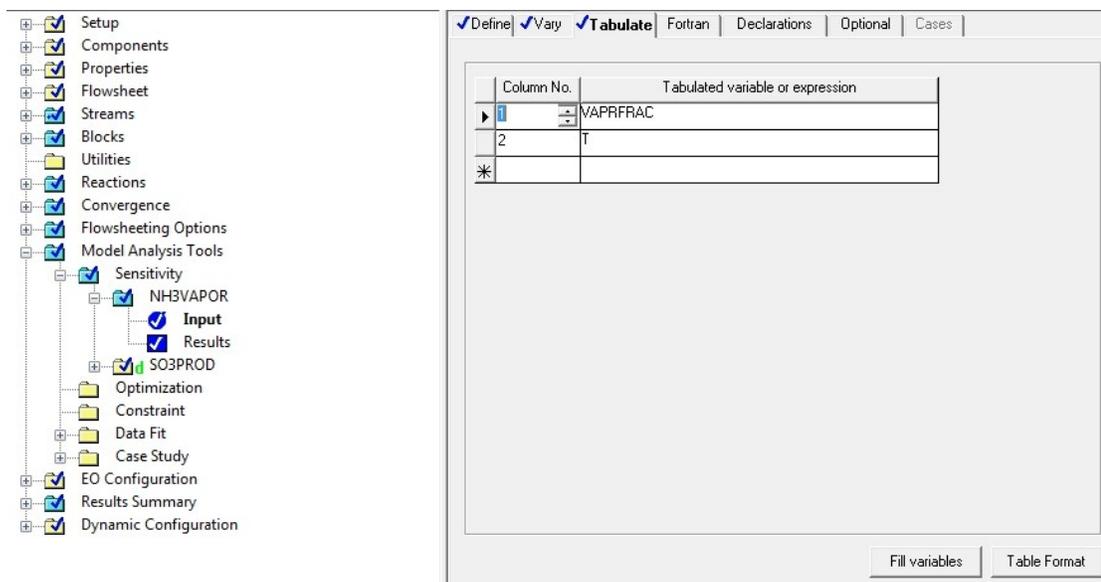


Figure 3.15: Shows how the defined variables were tabulated in NH3PROD.

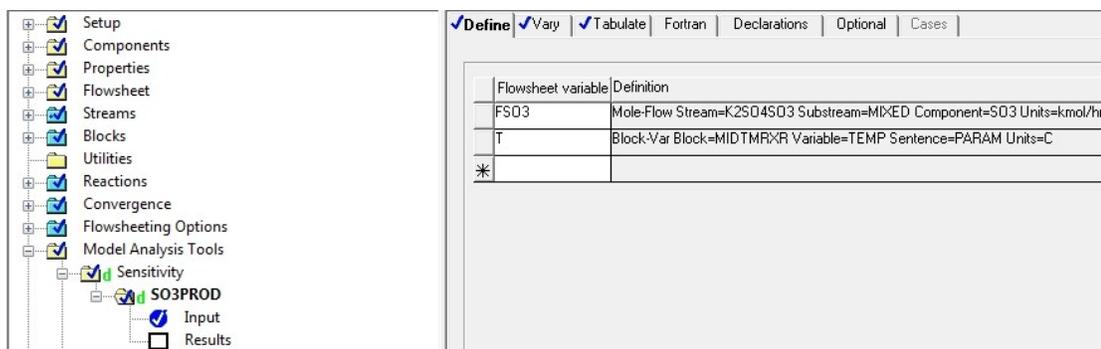


Figure 3.16: Shows the location of the sensitivity block SO3PROD and the definitions of the variables used.

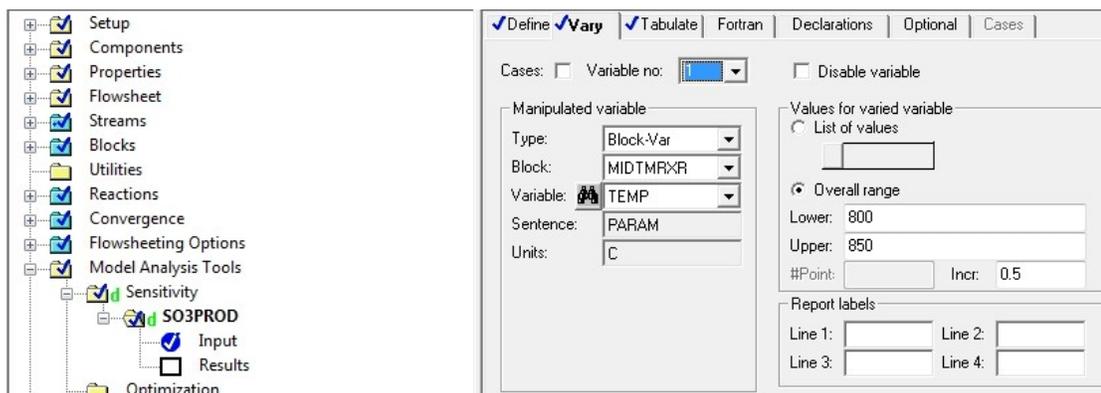


Figure 3.17: The temperature of the mid-temperature reactor was defined as the manipulated variable in SO3PROD, ranged from 800 to 850 °C, and incremented by 0.5 °C.

The screenshot displays a software interface with a tree view on the left and a tabulation table on the right. The tree view includes folders like Setup, Components, Flowsheet, Streams, Blocks, Utilities, Reactions, Convergence, Flowsheeting Options, Model Analysis Tools, Sensitivity, SO3PROD, Input, Results, Optimization, Constraint, Data Fit, Case Study, EO Configuration, Results Summary, and Dynamic Configuration. The right panel shows a table with columns 'Column No.' and 'Tabulated variable or expression'. The table contains two rows: row 1 with '1' and 'FSO3', and row 2 with '2' and 'T'. A third row with an asterisk is also visible. The 'Tabulate' option is checked in the top menu bar.

Column No.	Tabulated variable or expression
1	FSO3
2	T
*	

Figure 3.18: Shows how the defined variables were tabulated in SO3PROD.

References

- [1] "AspenTech." *Aspen Plus*®. N.p., n.d. Web. 21 June 2012.
<http://www.aspentech.com/products/aspentech-plus.aspx>
- [2] Lindberg, D., Backman, R., Chartrand, P., "Thermodynamic Evaluation and Optimization of the (Na₂SO₄ + K₂SO₄ + Na₂S₂O₇ + K₂S₂O₇) System," *Journal of Chemical Thermodynamics*, v.38, **2006**, p. 1568-1583
- [3] Turton, Richard, Richard C. Bailie, Wallace B. Whiting, and Joseph A. Shaeiwitz. *Analysis, Synthesis and Design of Chemical Processes*. Upper Saddle River, NJ: Prentice-Hall, **1998**

Chapter 4: Procedure and Error and Warning Analysis

To run the flow sheet in the current work, the user must have Aspen Plus[®] chemical process simulator version 7.2 or higher. Once the file has been opened in the program, access to all locations that have been discussed in this thesis are located in the data browser. Figure 4.1 shows the title of the final flow sheet (SA Process.apw) and where to access the data browser. There are two options to open the data browser. The first is to use the Data menu to choose individual options and the second is to click the “glasses” button to open the data browser window.

To run the simulation, the control panel is opened (highlighted in Figure 4.2). From the control panel, reinitializing the simulation may be required. If not, the simulation is simply started. Another method to run the simulation is to click the “Next” button (a blue “N” with a right-pointing arrow to its right also highlighted in Figure 4.2). A prompt will explain all required input is complete and ask to run the simulation. To run the simulation, “OK” is clicked.

Once the simulation has completed, the simulation results will display in the control panel. A total of 31 warnings (28 Physical Property and 3 Simulation) and 1 simulation error will be present. The physical property warning, shown in Figure 4.3, stated the correlation that was used to calculate the missing dielectric constant for SO₃. Figure 4.4 shows the next warning with 27 occurrences. This warning suggested that because the electrolyte model ENRTL-SR was in use, several physical property calculations would be incorrect. This warning was erroneous because calculations were performed and the calculated enthalpy values across the reactors were correct and within similar orders-of-magnitude. Without involving the complicated

thermodynamic models and numerical methods within Aspen Plus[®], these values were a good indication the calculations were correct.

The first simulation warning is shown in Figure 4.5. This warning simply stated the initial value of the design specification SO3CONV was below the lower bound and reset to a value slightly above that initial value. The last two simulation warnings are shown in Figure 4.6. These warnings stated that after the simulation had been reinitialized, there was zero feed to the electrolyzer and a heat exchanger. Notice the top of Figure 4.6 that this is the beginning of a convergence loop \$SOLVER01. Figure 4.7 shows \$SOLVER01 converged, negating any feed issues associated with these warnings.

Finally, the simulation error is also shown in Figure 4.6. This error was also located at the beginning of the convergence loop \$SOLVER01 which has been shown to converge in Figure 4.7.

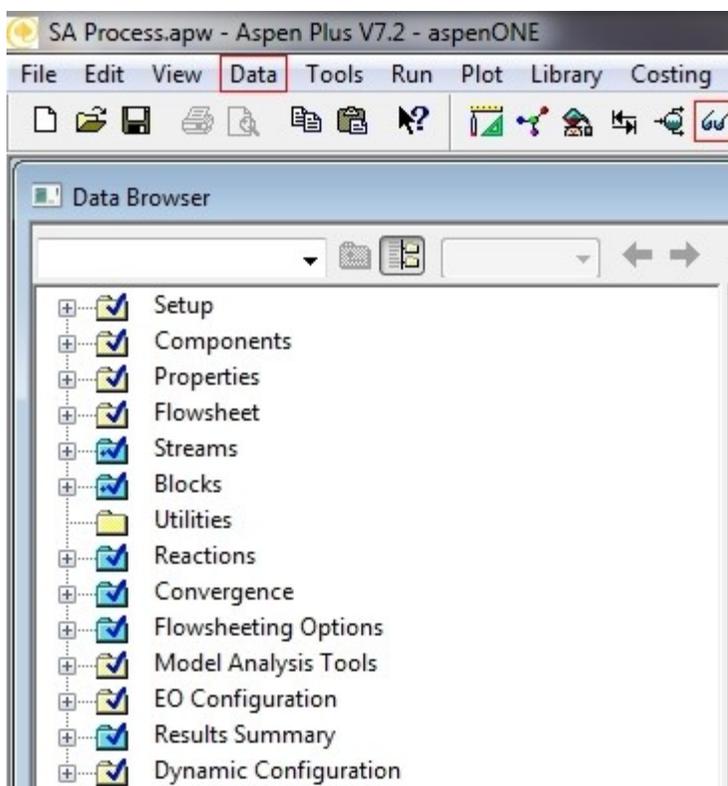


Figure 4.1: Shows how to open the data browser using the highlighted areas. The “Data” menu has the individual options displayed in the data browser window or the “glasses” button can be used to open the data browser window.



Figure 4.2: Location of the Control Panel button (left red highlight) and the “Next” button (right red highlight).

```
*
WARNING IN PHYSICAL PROPERTY SYSTEM
SYMMETRIC ELECTROLYTE NRTL MODEL GMENRILS HAS MISSING PARAMETERS:
Dielectric constant (CPDIEC) MISSING FOR SO3      . CPDIEC OF WATER
CALCULATED FROM HELGESON AND KIRKHAM CORRELATION (1974) WILL BE ASSUMED.
```

Figure 4.3: Physical property warning displayed in the control panel for missing dielectric constant (CPDIEC) for SO₃.

```
*
WARNING IN PHYSICAL PROPERTY SYSTEM
WATER IS NOT PRESENT IN THE STREAM. THE CALCULATED MIXTURE ENTHALPY
(HLMX), ENTROPY (SLMX), AND GIBBS FREE ENERGY (GLMX) ARE INCORRECT
WITH SYMMETRIC REFERENCE STATE FOR ELECTROLYTE SYSTEMS.
```

Figure 4.4: Physical property warning displayed in the control panel. This warning was repeated in 27 occurrences.

```

> Beginning Convergence Loop $OLVER03 Method: SECANT
*   WARNING
    INITIAL VALUE FOR DESIGN SPEC VARIABLE 1
    IS AT OR BELOW LOWER BOUND.
    VALUE = 0.00000
    LOWER BOUND = 0.100000E-02
    UPPER BOUND = 0.999000
    VARIABLE RESET TO 0.100800

```

Figure 4.5: Simulation warning displayed in the control panel for design specification SO3CONV.

```

>> Beginning Convergence Loop $OLVER01 Method: WEGSTEIN

Block: ELECFLSH Model: FLASH2
*   WARNING
    ZERO FEED TO THE BLOCK.  BLOCK BYPASSED

Block: $HX-3H02 Model: HEATER
*   WARNING
    ZERO FEED TO THE BLOCK.  BLOCK BYPASSED

Block: $HX-3HTR Model: MHEATER
**  ERROR
    HEAT STREAMS SUM TO ZERO DUTY.  BLOCK BYPASSED.

```

Figure 4.6: Simulation warning displayed in the control panel stating zero feed to two blocks in the flow sheet in the beginning of a convergence loop. Also contains the only simulation error displayed in the control panel which also converged in \$OLVER01 (refer to Figure 4.7).

```

>> Loop $OLVER01 Method: WEGSTEIN      Iteration    2
# Converged                          Max Err/Tol  -0.22050E-05

```

Figure 4.7: \$OLVER01 converged negating the warnings and error shown in Figure 4.6 and Figure 4.8, respectively. Convergence displayed in the control panel.

Chapter 5: Results and Discussion

5.1 Flow Sheet

Figure 1.3 is the complete and final flow sheet of the current work. Convergence was made difficult by the extensive recycle streams. To aid in convergence, two manual tear streams were placed within the flow sheet. One tear stream was the ammonium sulfate stream (AM_2SO_4), which is the outlet of the electrolyzer and the inlet of the low temperature reactor, after the heat exchanger HX-3. And the other tear stream was the potassium sulfate stream (K_2SO_4), which was the outlet of the sulfur trioxide separator and the inlet of the low temperature reactor.

Design specifications were placed in the flow sheet to aid in the convergence as well. The design specification H₂O-MU was used to calculate the water feed to compensate for the losses after the hydrogen product flash. The design specification SO₃CONV was used to determine the conversion of potassium pyrosulfate at the constant process pressure of 9 bar. Refer to Section 3.2.4 for more details on the design specifications and to Section 5.6 for the results.

5.2 Energy and Mass Balance

Figure 5.1 is a simplified process flow diagram that represents an Aspen Plus[®] model of a design for the SA solar thermochemical hydrogen production process. The operating pressure is 9 bar and energy is recovered from the ammonia/water vapor stream from the low temperature reactor R-2 by expansion through a condensing turbine/generator set, H-1 and G-2 in Figure 5.1, respectively. Not shown are the liquid ammonia/water repressurization pump and other details.

Table 5.1 shows the energy and mass balance of the simplified design of the SA solar thermochemical hydrogen production plant.

Table 5.1: Energy and mass balance based on the plant design. Refer to Figure 5.1 for definitions of $Q_1 - Q_3$ in the plant.

<u>Energy Balance [MW]</u>		<u>Mass Balance [kg/hr]</u>	
<u>Energy In</u>		<u>Mass In</u>	
Low Temp. Reactor Solar Thermal Input	999	Feed Water	101,013
Mid Temp. Reactor Solar Thermal Input	469	Total:	101,013
High Temp. Reactor Solar Thermal Input	153	<u>Mass Out</u>	
Feed Water	0	Hydrogen Product	11,111
Electricity Import	69	Oxygen Product	89,902
Total:	1,691	Total:	101,013
<u>Energy Out</u>		<u>% Subtotal</u>	<u>Performance Summary</u>
Ammonia/Water Condenser (Q_1)	812	65	Overall Efficiency [%]
Heat Losses from Electrolyzer (Q_2)	391	31	
Absorber Separator (Q_3)	36	3	
Hydrogen Product Separator	6	1	
Oxygen Product	0	0	
Subtotal:	1,245		
Hydrogen Product	446		
Total:	1,691		

The design was based on a flow sheet that had no manual tear streams. Values are based on production of 133,333 kg/day of 300 psig hydrogen with the plant operating 12 hours per day. With a plant capacity factor of 75% this results in an average production rate of 100,000 kg/day. The enthalpies were obtained from Aspen Plus[®] on the basis of the higher heating value (HHV) of hydrogen, approximately 437 MW. Another possible basis was the lower heating value (LHV) of hydrogen, approximately 370 MW. With this value a STCH efficiency, as defined in Eq. 5.1, of 22% was calculated.

Table 5.2 shows the values obtained directly from the current work, Figure 1.3.

Table 5.2: Energy and mass balance based on the current work.

Energy Balance [MW]		Mass Balance [kg/hr]	
<u>Energy In</u>		<u>Mass In</u>	
Low Temp. Reactor Solar Thermal Input	995	Feed Water	94,283
Mid Temp. Reactor Solar Thermal Input	449	Ammonium Sulfate (Manual Tear)	1,558,430
High Temp. Reactor Solar Thermal Input	147	Potassium Sulfate (Manual Tear)	7,944,350
Potassium Sulfate (Manual Tear)	-17,150	Total:	9,597,063
Ammonium Sulfate (Manual Tear)	-5,304		
Feed Water	-419	<u>Mass Out</u>	
Pump-1	0	Ammonium Sulfate (Manual Tear)	1,662,190
Pump-2	0	Potassium Sulfate (Manual Tear)	7,838,150
Electrolyzer Power Requirement	226	Hydrogen Product	10,640
Heat Pump Electrical Requirement	85	Oxygen Product	86,090
H ₂ Product Compressor	5	Separated Liquid from Hydrogen Product	10,009
Total:	-20,964	Total:	9,597,070
<u>Energy Out</u>		<u>Difference [%]</u>	
Ammonia/Steam Condenser	778		0.00
Heat Pump Motor	85		
Heat Losses from Electrolyzer	237		
Absorber Separator	34		
Electrolyzer Flash	52		
Hydrogen Product Separator	6		
Mid-Temperature Reactor Separator	0		
Potassium Sulfate (Manual Tear)	-17,000		
Ammonium Sulfate (Manual Tear)	-5,431		
Turbine/Generator Electrical Power	248		
Oxygen Product	3		
Hydrogen Product	9		
Total:	-20,979		
Difference [%]	0.07		

The enthalpies were based on an elemental reference state where the enthalpy is zero for the elements in their standard state at 25 °C. This standard state is used by Aspen Plus[®] so that reaction enthalpies are computed automatically from reaction stoichiometry. The electrolyzer power requirements were based on a voltage of 0.8 V, a value obtained from Electrosynthesis Company, Inc. The absorber separator is

located after the chemical absorption step to separate the oxygen from the aqueous sulfite stream. The enthalpy change across this block was associated with the heat of condensing the water vapor that comprises a majority of the product stream from the absorber. The electrolyzer flash is located after the electrolysis step to separate the hydrogen product from the aqueous sulfate stream. The enthalpy change across the block was associated with cooling the outlet of the electrolyzer. The hydrogen product separator produces a pure hydrogen outlet stream. The majority of bottoms for this block was composed of water. Therefore, in the energy balance column, the enthalpy of this liquid bottoms outlet stream was deducted from the feed water inlet and, in the mass balance column, the mass flow was deducted from the feed water. The enthalpy change was associated with condensing water vapor in the H₂ product.

The percent of subtotal column in Table 5.1 refers to the fraction of enthalpy out with respect to the total excluding the enthalpy of the hydrogen stream. It is clear the greatest heat losses occur for condensing the ammonia/water stream (Q_1 where Q is regarded as a heat loss here) and from the electrolyzer (Q_2). To increase the efficiency of the process, optimization in these two areas would produce significant results.

For complete stream tables, refer to Appendix C.

5.3 Solar Reactors and the Chemical Absorber

The low, mid, and high temperature reactors use heat from solar energy to drive their respective reactions. The low and high temperature reactors were modeled using the Gibbs reactor (RGibbs) while the mid-temperature reactor used the

stoichiometric reactor (RStoich). Section 3.2 describes, in more detail, these reactor blocks.

Table 5.3 shows a summary of the results of the low temperature reactor.

Table 5.3: Summary of the low temperature reactor results.

RGibbs Results	
Outlet Temperature [°C]	400
Outlet Pressure [bar]	9
Heat Duty [Watt]	995233098
Net Heat Duty [Watt]	995233098
Vapor Fraction	0.65376634

Laboratory results showed that 400 °C was a reasonable temperature to keep the molten salt streams liquid and to evolve the ammonia vapor. The pressure of 9 bar was used previously by FSEC but the high pressure was necessary for the electricity generation portion of the flow sheet. The high temperature/high pressure ammonia/water stream was sufficient to supply the electrolysis its required amount of electricity from the work from the steam turbine. For more detailed results of the power generation, and an alternative low pressure system, refer to Section 5.5. The heat duty displays the calculated heat duty for the block while the net heat duty displays the calculated net duty if there was an inlet heat stream. There were no inlet heat streams for any of the solar reactors. Table 5.4 shows the mass and energy balance of the low temperature reactor.

Table 5.4: Mass and energy balance of the low temperature reactor.

Total	In	Out	Generated	Relative Difference
Mole Flow [kmol/hr]	84892	96281.8	11389.8	0
Mass Flow [kg/hr]	9502785.58	9502785.58	0	8.9969e-14
Enthalpy [Watt]	-2.245e+10	-2.245e+10	0	-1.699e-16

The generated column shows the ammonia generation in this portion of the flow sheet. The error tolerance was defined automatically by Aspen Plus[®] as 10^{-4} and as long as the relative difference was less than that specified tolerance within a certain maximum number of iterations, the mass balance was said to have converged. Table 5.5 shows the phase compositions for the low temperature reactor.

Table 5.5: Phase composition of the ammonia and molten salt outlet streams of the low temperature reactor.

Phase	Vapor	Liquid
Phase Fraction	0.65376634	0.34623366
Outlet Stream	NH3-HOT	K2S2O7
Total Flow [kmol/hr]	62945.8	33336
Component	Mole Fraction	Mole Fraction
H2O	0.81905385	0
K2S2O7	0	0.95833333
NH3	0.17653283	0
SO2	0.00441332	0
K2SO4	0	0.04166666

Table 5.6 shows a summary of the results of the mid-temperature reactor.

Table 5.6: Summary of the mid-temperature reactor results.

RStoich Results	
Outlet Temperature [°C]	834.5
Outlet Pressure [bar]	9
Heat Duty [Watt]	449373420
Net Heat Duty [Watt]	449373420
Vapor Fraction	0.16533323

The temperature of 834.5 °C was acquired from a combination of information input into a design specification and a sensitivity analysis performed. At the constant pressure of 9 bar and the equilibrium data from [1], this was the temperature at which a sufficient amount of SO₃ was evolved for the required amount of hydrogen production. Refer to Section 5.6 for more details on the results of the SO₃CONV

design specification associated with the mid-temperature reactor. Table 5.7 shows the mass and energy balance of the mid-temperature reactor.

Table 5.7: Mass and energy balance of the mid-temperature reactor.

Total	In	Out	Generated	Relative Difference
Mole Flow [kmol/hr]	33336	39940.7385	6604.73848	-1.822E-16
Mass Flow [kg/hr]	8366949.02	8366949.02	0	1.1131E-16
Enthalpy [Watt]	-1.806E+10	-1.806E+10	0	2.1123E-16

The generated column shows the sulfur trioxide generation in this portion of the flow sheet. Table 5.8 shows the vapor-liquid (VL) equilibrium results for the mid-temperature reactor.

Table 5.8: VL equilibrium results for the mid-temperature reactor.

Component	F	X	Y	K
K2SO4	0.20013998	0.23978429	4.2932e-81	1.7905e-80
K2S2O7	0.63449657	0.7601795	3.5731e-79	4.7003e-79
SO3	0.16536345	3.6216e-05	1	27612.3646

In Table 5.8, F is the mole fraction of combined phases of the total product stream, X is the equilibrium liquid mole fraction in the product at outlet conditions, Y is the equilibrium vapor mole fraction in the product at outlet conditions, and K is the VL equilibrium Y/X of the product at outlet conditions.

Table 5.9 shows a summary of the results of the high temperature reactor.

Table 5.9: Summary of the high temperature reactor results.

RGibbs Results	
Outlet Temperature [°C]	1000
Outlet Pressure [bar]	9
Heat Duty [Watt]	146973430
Net Heat Duty [Watt]	146973430
Vapor Fraction	1

The temperature of 1000 °C was a manual input value chosen because of the high temperature required for the decomposition of SO₃. Table 5.10 shows the mass and energy balance of the high temperature reactor.

Table 5.10: Mass and energy balance of the high temperature reactor.

Total	In	Out	Generated	Relative Difference
Mole Flow [kmol/hr]	6604.73848	9295.16305	2690.42457	0
Mass Flow [kg/hr]	528803.103	528803.103		-1.101E-15
Enthalpy [Watt]	-604073074	-604073074		0

The generated column shows the oxygen generation in this portion of the flow sheet.

Table 5.11 shows the phase compositions for the high temperature reactor.

Table 5.11: Phase composition of the outlet stream of the high temperature reactor.

Phase	Vapor
Phase Fraction	1
Outlet Stream	NH3-HOT
Total Flow [kmol/hr]	9295.16305
Component	Mole Fraction
SO3	0.13166949
SO2	0.57888701
O2	0.2894435

Table 5.12 shows a summary of results of the chemical absorber.

Table 5.12: Summary of the chemical absorber results.

RStoich Results	
Outlet Temperature [°C]	162.427263
Outlet Pressure [bar]	9
Heat Duty [Watt]	0
Net Heat Duty [Watt]	0
Vapor Fraction	0.10671718

The reactor was manually set as adiabatic for full use of the heat of reaction in the outlet stream. The heat has to exit the reactor by increasing the temperature of the

ammonium sulfite stream which was then used to preheat the ammonia inlet stream.

Table 5.13 shows the mass and energy balance of the chemical absorber.

Table 5.13: Mass and energy balance of the chemical absorber.

Total	In	Out	Generated	Relative Difference
Mole Flow [kmol/hr]	72240.5632	55572.5632	-16668	2.0144e-16
Mass Flow [kg/hr]	1664639.66	1664639.66		0
Enthalpy [Watt]	-4.847e+09	-4.847e+09		-2.277e-06

The generated column shows the use of the ammonia from the inlet stream. Table 5.14 shows the VL equilibrium results for the chemical absorber.

Table 5.14: VL equilibrium results for the chemical absorber.

Component	F	X	Y	K
H2O	0.8277466	0.86460417	0.519228	0.60053331
AM2SO3	0.09997739	0.11192132	1.7247e-95	1.857e-107
SO3	0.02203765	0.01946337	0.04358587	2.2392902
SO2	0.00183272	0.00194616	0.00088319	0.45383789
O2	0.04840562	0.00206497	0.43630293	211.267508

5.4 Pinch Analysis and Heat Integration

Heat integration was a crucial part of the current work. To keep the efficiency at a sufficient value, useable heat from process streams needed to be exchanged to those that required heating or where it would be useful to increase the temperature prior to entering a reactor. A standard pinch analysis algorithm from [2] was utilized as a preliminary source of a heat integration system. The pinch analyses performed with these algorithms are almost never the optimum economic design but it does represent a good starting point [2]. Hence, after working on this project, more efficient means of heat integration became clear.

A pinch analysis spreadsheet from [3] was used along with the algorithm from [2]. The spreadsheet allowed for a check of the hand calculations and vice versa. The spreadsheet allows the user to choose an input method. In this instance, the mass flow rate and the specific heat capacity were used because these two values were readily available after Eq. 3.6 was used to find C_p [J/kg·K] for the streams of interest in heat exchange. A global ΔT_{\min} of 20 °C was chosen. Table 5.15 shows the input and results of the pinch spreadsheet.

Table 5.15: Input and results of the pinch analysis spreadsheet from [2]. Columns “Stream Name” through “Specific Heat Capacity” were input and the remaining columns were results of the calculations done within the spreadsheet.

Stream Name	Supply Temp.	Target Temp.	Mass Flow Rate	Specific Heat Capacity	Heat Flow	Steam Type	Supply Shift	Target Shift
	°C	°C	kg/s	kJ/kg·K	kW	Hot/Cold	°C	°C
SFITPRD2	162	108	4.38E+02	5.10	121,000	HOT	152	98
SO2-O2	1,000	147	1.47E+02	0.273	34,200	HOT	990	137
NH3-C3	-4	88	3.16E+02	4.99	145,000	COLD	6	98
AM2SO4-2	100	200	4.62E+02	2.64	122,000	COLD	110	210
K2S2O7	400	785	2.32E+03	5.99E-03	5,360	COLD	410	795
SO3-2	835	980	1.47E+02	0.965	20,500	COLD	845	990

Using the results above, shifted and non-shifted temperature composite curves and a grand composite plot were generated and are shown in Figures 5.2, 5.3, and 5.4, respectively. Hot streams (red) are those releasing energy (heat) and being cooled down and cold streams (blue) are those accepting energy and being warmed up.

Again, these pinch analyses are good starting points for heat integration.

However, the placement of the heat exchangers in this work was done by engineering judgment and experience gained while working on the project. The placement of heat exchangers in the flow sheet, shown in Figure 1.3, labeled with HX then a number 1 through 4, made significant use of the heat throughout the plant.

5.5 Power Generation

Power generation was possible in this process by recovery of the large amount of heat required to vaporize the complete amount of water from the low temperature reactor. Further along in the process, this steam/ammonia mixture would need to be condensed before entering the absorber. As opposed to rejecting and wasting that useful energy, the high pressure/high temperature stream was run through a single-flow condensing turbine (labeled TURBINE in the flow sheet Figure 1.3) and the work out was assumed to have 100% electrical power recovery.

The steam/ammonia stream enters the turbine at 9 bar and 400 °C. The single-flow condensing unit allowed the inlet stream to expand from the inlet pressure to a pressure less than atmospheric where the outlet pressure was maintained by a condenser [4]. The outlet pressure of the turbine was 0.08 bar. An efficiency of 0.85 was defined for the isentropic turbine. Table 5.16 displays the results of the turbine.

Table 5.16: Results of the single-flow condensing turbine (TURBINE).

TURBINE Results	
Inlet Temperature [°C]	400
Inlet Pressure [bar]	9
Outlet Temperature [°C]	43
Outlet Pressure [bar]	0.08
Vapor Fraction	0.97244275
Net Work [Watt]	248476826

Setting the exhaust pressure at a sub-atmospheric pressure gives a large amount of work. However, the exiting vapor stream still required condensing. The condenser (CONDENSE) was set to have a vapor fraction of zero. The amount of work required for the “heat pump” motor was approximately 85 MW and the outlet temperature was -4 °C. To reach this low temperature, refrigerant would be needed

and because the plant will most likely be located in the desert, this low temperature presents an issue. Also, when this value was taken into account with the electricity generated, there was a need to import electricity from the grid to run the electrolyzer and the condenser. This had the effect of decreasing the efficiency of the plant, as defined by Eq. 5.1, to 22%.

An alternative exists for power generation within the plant. A steam power plant has been designed by Dr. Lloyd C. Brown, a consultant on the project from TChemE Solutions. The Rankine steam power plant exchanged heat from high temperature streams throughout the process (i.e. the steam/ammonia stream originally run through the turbine) to produce steam to run a standard steam power plant. This plant produced approximately 260 MW. This alternative would allow a reduction of the system pressure to, at or slightly above, the minimum pressure in the electrolyzer. It would also require multiple heat exchangers, turbines, and a compressor. Therefore, there are cost trade-offs to be considered when deciding between the turbine and steam power plant modes of power generation.

Designing alternate modes of power generation was compelled by the high pressures required in the current work, namely for the three solar reactors. Because each solar reactor has gas evolution, a higher pressure would require a higher temperature to drive the reaction to a point where the conversion of the reactant is sufficient. This can be seen in the current work around the mid-temperature reactor. This reactor uses thermodynamics from [1] via the design specification SO3CONV making this the only reactor in the flow sheet that is affected by pressure as the model stands now.

To see the effects of pressure on the mid-temperature reactor, refer to the work done by Wang where RGA data for the decomposition of a mixture of molten salts is shown. This work shows the evolution of SO_3 occurring between 500 °C and 700 °C [5]. This is in contrast with the necessary temperature of 835 °C for the mid-temperature reactor in the current flow sheet. Wang's experiments were performed at atmospheric pressure while the system pressure in the Aspen Plus[®] flow sheet was 9 bar. This increase in pressure causes the necessary temperature to increase (refer to Section 5.8). Changes in pressure will not affect any of the other reactors in this flow sheet because no thermodynamic data or kinetics were used to design them.

5.6 Values from Design Specifications

H2O-MU and SO3CONV were the two design specifications used in the flow sheet to determine the water make-up required due to the loss by the hydrogen product stream and the conversion within the mid-temperature reactor using digitized laboratory results from [1], respectively.

Section 3.2.4 describes the H2O-MU design specification set-up. H2O-MU increased the feed water as a make-up of the lost water vapor from the exit streams by equalizing water flow rate at two points in the plant. Table 5.17 shows the results of H2O-MU.

Table 5.17: Results of the H2O-MU design specification.

Variable	Initial value	Final value	Units
Manipulated: H2O-FEED	5556	5789.10546	kmol/hr
WH2O1	46000	46000	kmol/hr
WH2O2	45766.851	45999.0777	kmol/hr

The variable column in the table above displays the defined variables in the design specification. The initial value displays either the value of the particular variable defined by the designer, in this work H2O-FEED and WH2O1, or the value calculated by Aspen Plus[®], WH2O2. The final value was used for the simulation and overwrote any initial value. The initial input value of the water feed was set to the stoichiometric amount required because the molar ratio of water to hydrogen produced is 1:1. However, with a loss from the hydrogen product stream, the water feed must be increased to compensate for that loss; which is shown by the ~230 kmol/hr increase in Table 5.17. It may be possible to recycle this water into the ammonium sulfate stream to the low temperature reactor once it is separated. This would decrease the amount of make-up water required.

Section 3.2.4 describes the SO3CONV design specification set-up.

SO3CONV varied the conversion of potassium pyrosulfate to equalize equilibrium thermodynamics with a laboratory phase diagram to account for pressure effects on the mid-temperature reactor. Table 5.18 shows the results of SO3CONV.

Table 5.18: Results of the SO3CONV design specification.

Variable	Initial value	Final value	Units
Manipulated: Conversion of $K_2S_2O_7$	0.1008	0.20674049	
XK ₂ SO ₄	0.12608669	0.20013998	
P	9	9	bar

The initial value of the conversion of $K_2S_2O_7$ was determined by Aspen Plus[®] but then overwritten with the final value due to the phase diagram information supplied by the design specification. The initial and final values of the mole fraction of K_2SO_4 (XK2SO4) correspond to the differing values of the conversion of $K_2S_2O_7$.

5.7 Values from Calculator Blocks

ELECPOWR and PLANTEFF were the two calculator blocks used in the flow sheet to calculate the heat duty required by the electrolyzer dependent on the amount of hydrogen produced and the overall efficiency of the process, respectively.

Section 3.2.5 describes the ELECPOWR calculator block set-up.

ELECPOWR used the amount of hydrogen produced FH2 [kmol/hr] to calculate the electrical power requirement of the electrolyzer based on a voltage of 0.8 V. Table 5.19 shows the results of ELECPOWR.

Table 5.19: Results of the ELECPOWR calculator block.

Variable	Value read	Value written	Units
FH2	5278.09397		kmol/hr
ELECPOWR	226336418	226336399	Watt

Based on the amount of hydrogen produced, the electrolyzer would require approximately 226 MW of electrical power. This value was exported to an input heat stream to the electrolyzer to simulate the power input to the reactor. Table 5.20 shows a summary of the results of the electrolyzer.

Table 5.20: Summary of the electrolyzer results.

RStoich Results	
Outlet Temperature [°C]	130
Outlet Pressure [bar]	9
Heat Duty [Watt]	-24154885
Net Heat Duty [Watt]	-250491284
Vapor Fraction	0.13171015

The temperature of 130 °C was manually entered and based on information acquired from Electrosynthesis Company, Inc. Because there is an input heat stream on the electrolyzer, the heat duty and net heat duty values are different. Physically, this

represents the heat loss from the electrolyzer. The heat input was approximately 226 MW added to approximately 24 MW of lost heat gives the ~250 MW shown in Table 5.20. Table 5.21 shows the mass and energy balance of the electrolyzer.

Table 5.21: Mass and energy balance of the electrolyzer.

Total	In	Out	Relative Difference
Mole Flow [kmol/hr]	58673.6687	58673.6687	1.2401e-16
Mass Flow [kg/hr]	1682878.14	1682878.14	-1.384e-16
Enthalpy [Watt]	-5.244e+09	-5.244e+09	-2.252e-10

Table 5.22 shows the vapor-liquid equilibrium results for the electrolyzer.

Table 5.22: VL equilibrium results for the electrolyzer.

Component	F	X	Y	K
H2O	0.79273942	0.86752453	0.23444002	0.27024023
AM2SO3	0.00473466	0.00536887	9.268e-110	3.9904e-94
AM2SO4	0.08995858	0.10200868	1.15e-109	2.6069e-95
SO3	0.02085926	0.02314436	0.00380007	0.16419
SO2	0.00174949	0.00195086	0.00024614	0.12617377
H2	0.08995858	2.6835e-06	0.76151375	283780.115

Section 3.2.5 describes the PLANTEFF calculator block set-up. PLANTEFF used several parameter values from the flow sheet to calculate the overall efficiency of the plant based on the amount of hydrogen produced. Table 5.23 shows the results of PLANTEFF.

Table 5.23: Results of the PLANTEFF calculator block.

Variable	Value read	Value written	Units
ELECPOWR	226336399		Watt
TURBWORK	-248476826		Watt
FH2	5278.09397		kmol/hr
HEATTOT	-1.59E+09		Watt
ETA		0.22592122	
LHV		354569686	Watt

The variable column displays the defined variables of the design specification. The value read column displays values from the simulation needed to calculate the

efficiency. The value written column displays the value of the variable determined by the calculator block. The two values determined by the calculator block were the efficiency of the plant ETA and the lower heating value of hydrogen LHV [Watt]. Based on the approximately 130,000 kg/day H₂ produced, the efficiency of the plant was determined to be 23%. Refer to Section 5.9 for details on the efficiency calculation.

5.8 Values Obtained from Sensitivity Analyses

NH₃VAPOR and SO₃PROD were the two sensitivity analyses performed on the flow sheet to determine, at constant pressure, the temperature just before the NH₃-water stream vaporized and the temperature at which the necessary amount of SO₃ was produced in the mid-temperature reactor, respectively.

Section 3.2.6 describes the NH₃VAPOR sensitivity analysis set-up. This sensitivity analysis was performed because with the SO₂/O₂ vapor stream and the NH₃/water stream entering the absorber, the NH₃/water stream should have a mostly liquid fraction for greater ease of reaction. Fortunately, at the pressure of 9 bar, the NH₃/water stream stays condensed up to, and perhaps greater than, the peak temperature used in this sensitivity analysis, 150 °C. Figure 5.5 shows the upper portion of the results from this analysis. Because of the results of this analysis, the heat exchanger, used to exchange heat between the -4 °C NH₃/water stream and the product of the absorber after oxygen separation (SFITPRD2), was set to 88 °C to avoid a temperature crossover.

Section 3.2.6 describes the SO₃PROD sensitivity analysis set-up. This sensitivity analysis was performed to determine the temperature at which the mid-temperature reactor should run, at constant pressure, with the phase diagram information from [1] incorporated into the reactor via the design specification SO₃CONV. Intermediate results of the analysis are shown in Figure 5.6. This analysis was very special because of its results. As can be seen, there are errors and warnings associated with the conclusion of this analysis. Temperature ranges of 831 °C to 833.5 °C and 836.5 °C to 837.5 °C show either errors or warnings in model convergence. However, the model converged satisfactorily for temperature range of 834 °C to 836 °C. One must also notice the flow of H₂ in the FH2 column. In the converged temperature range, the appropriate amount of H₂ is produced. After this sensitivity analysis was conducted, a temperature of 834.5 °C was chosen for the temperature of the mid-temperature reactor. Figure 5.7 shows a plot of the flow rate of SO₃ [kg/hr] versus the temperature of the mid-temperature reactor. It shows that the flow rate increases with increasing temperature and that a sufficient amount of SO₃ (approximately 53,000 kg/hr) is produced at about 830 °C. This temperature is higher than what would be expected from laboratory data. This is due to the elevated pressure of this process. To evolve the SO₃ vapor at higher than atmospheric pressure, the temperature must increase. A lower system pressure has been discussed in Section 5.5.

These sensitivity analysis results are a pertinent part of the usefulness of this preliminary flow sheet. Using the flow sheet, sensitivity analyses and optimization

studies can all be completed after any changes are made to the process. These analyses and studies can be found under Model Analysis Tools in the data browser.

5.9 Efficiency

The efficiency of the plant is based on a definition set forth by the DOE. Eq. 5.1 is the definition of the efficiency.

$$\eta = \frac{-\Delta H_{[f(H_2O)_g]}[Watt]}{Q[Watt]+E[Watt]} \quad (5.1)$$

The numerator is the heat of formation of gaseous water to liquid water dependent upon the amount of hydrogen produced with units of Watts. The denominator is the total heat Q [Watt] necessary for the three main solar reactors and the electrolyzer plus the imported electricity from the grid E [Watt]. Using the values of the combined required heat of the three solar reactors, the electrical power requirement of the electrolyzer, the work output of the turbine, and amount of hydrogen produced, an efficiency of 23% was calculated.

5.9.1 LHV of Hydrogen

Because the definition of the efficiency was put forth by the Department of Energy, a conversion factor from the DOE website [6] was used to calculate the LHV of hydrogen. The conversion used to calculate the efficiency for this process was 119.96 MJ/kg H₂. See Appendix B for calculation of conversion factor pertinent to this process. Using the conversion factor and a time basis of a 12 hour day, the LHV was found to be approximately 355 MW.

5.9.2 Total Heat (Q) and Import Electricity (E)

The total heat consists of the heats of the high, medium, and low temperature solar reactors along with the electrical power needed in the electrolyzer. The power requirement for the electrolyzer is offset by the work done by a power recovery system in the process. In this work, a turbine produces electricity from the high temperature/high pressure vapor ammonia/water stream. The amount of work produced by the turbine (~250 MW) is greater than the electricity requirement of the electrolyzer (~226 MW) and the excess can supply heat, via a resistive heating element, for the high temperature reactor. However, this should be investigated in future work as it was not in this study. Because the electricity generation from the turbine was greater than the need of the electrolyzer, E [Watt] was equal to zero.

Combining the total heat requirement for the solar reactors and the electrical requirement of the electrolyzer via a heat mixer block in Aspen Plus[®] (QMIXER MIXER) showed a total of 1.59 GW (Q). The efficiency calculation takes place in a calculator block labeled PLANTEFF. The calculator block uses the molar flow of hydrogen produced (5,278 kmol/hr) from the electrolyzer and, using the conversion factor stated earlier, converts that number to the LHV needed. The combined output power stream and converted LHV is then used in the efficiency calculation.

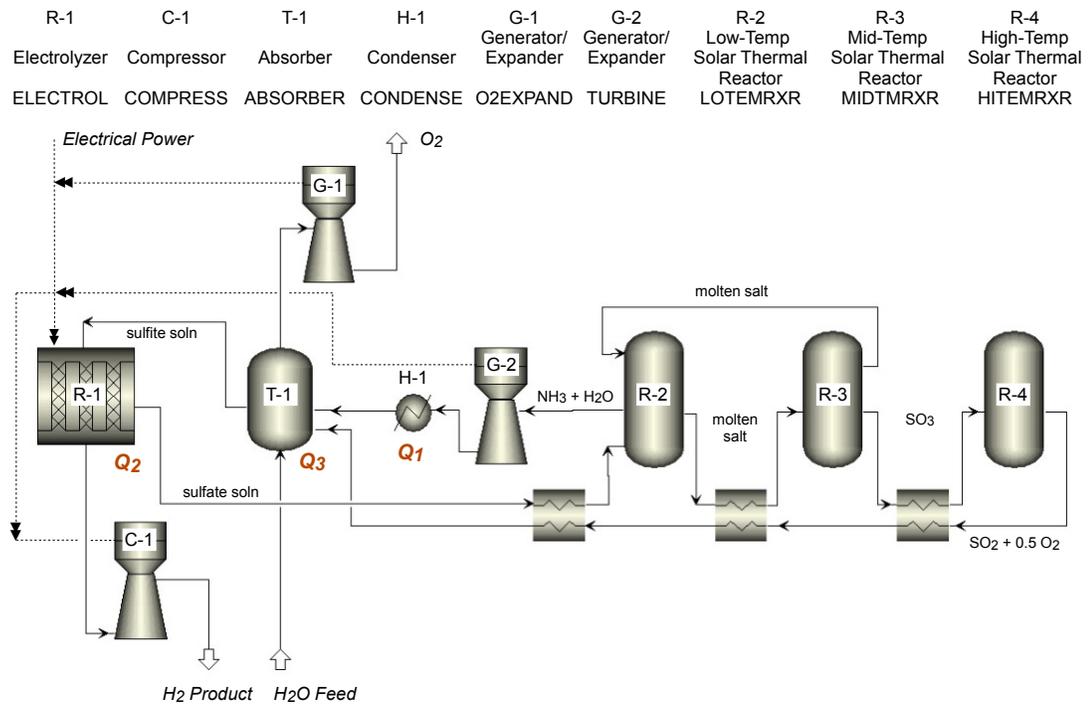


Figure 5.1: Simplified process flow diagram of the solar thermochemical hydrogen plant. Refer to Table 5.1 for use of $Q_1 - Q_3$ in the energy balance.

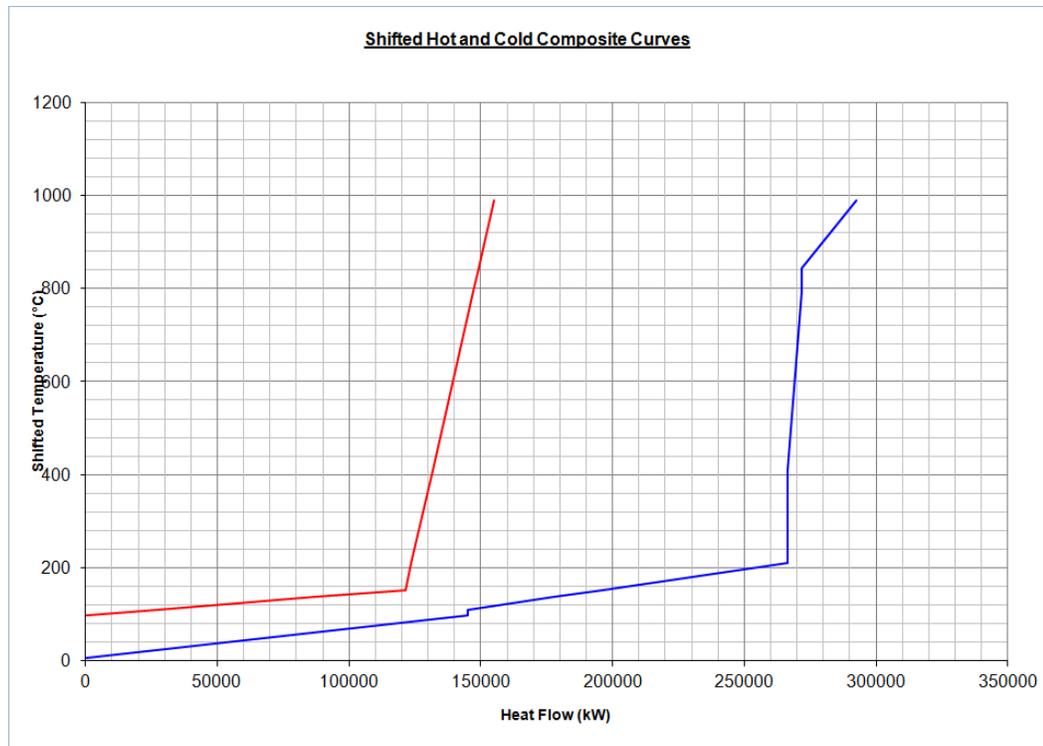


Figure 5.2: Shifted temperature composite curve generated from a standard pinch analysis procedure where the red line represents the hot streams and the blue line represents the cold streams.

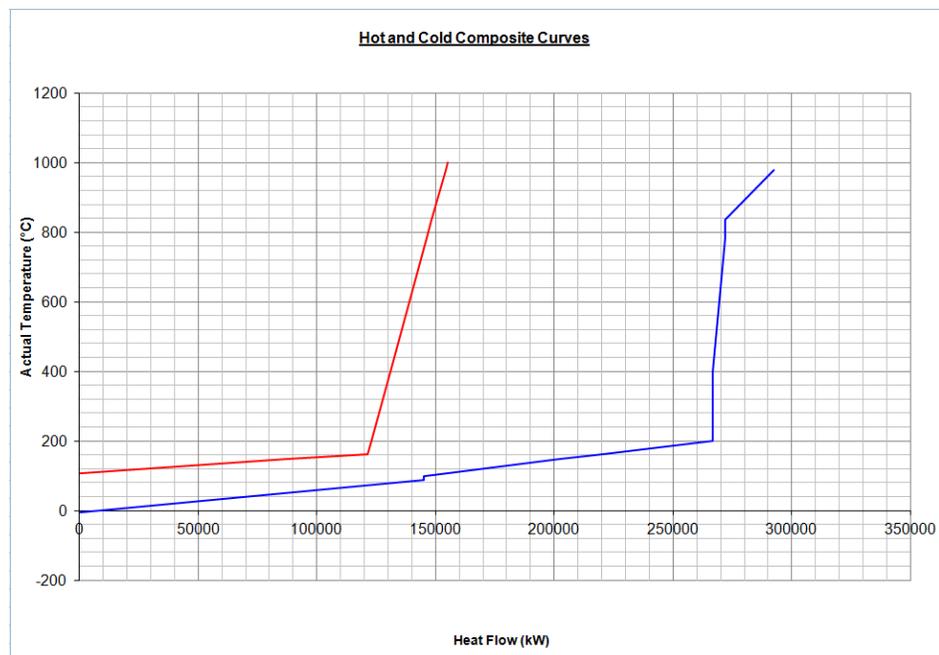


Figure 5.3: Non-shifted temperature composite curve generated from a standard pinch analysis procedure where the red line represents the hot streams and the blue line represents the cold streams.

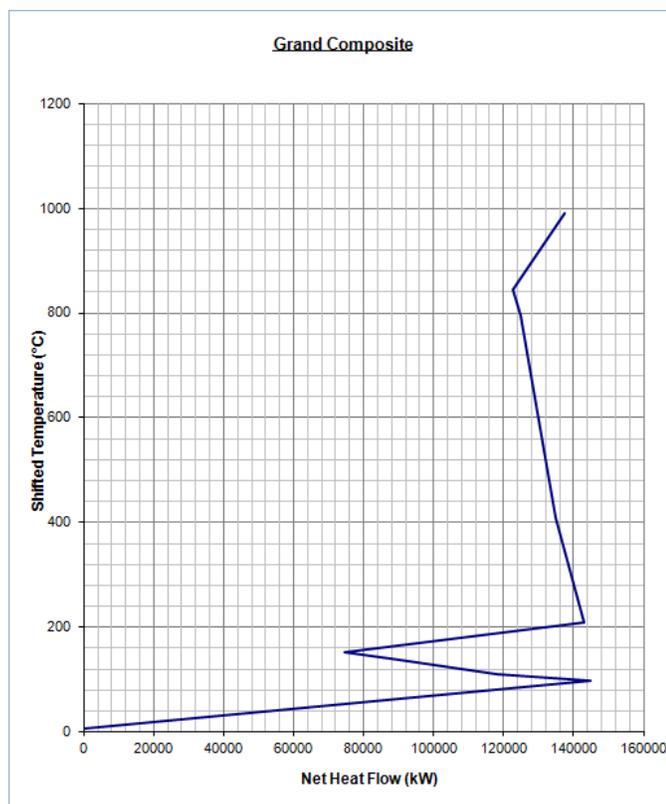


Figure 5.4: A grand composite curve generated from a standard pinch analysis procedure.

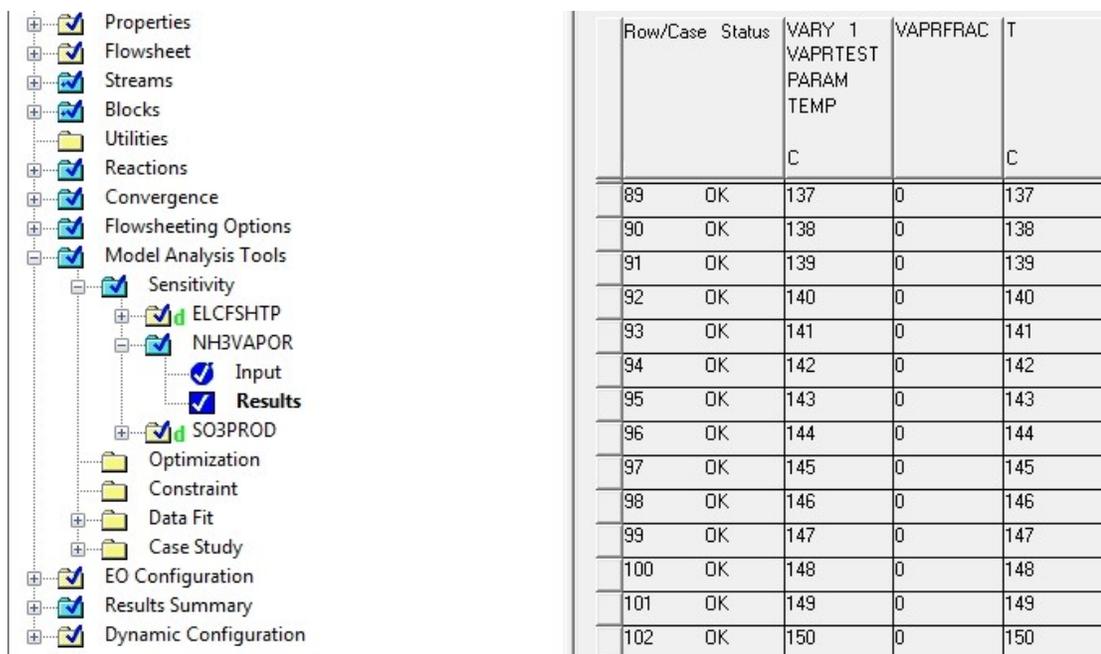
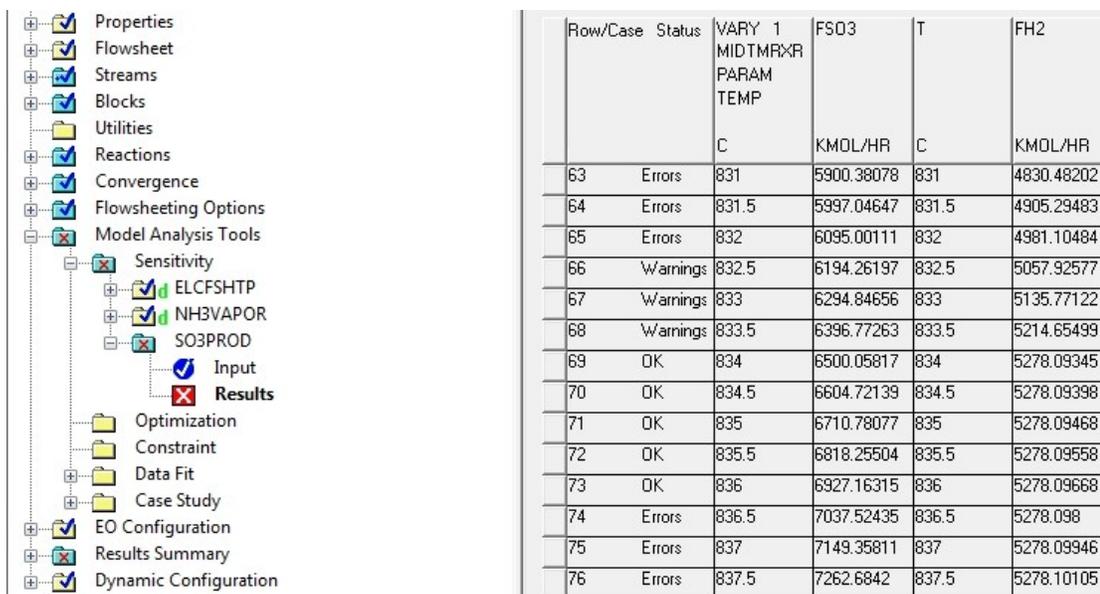


Figure 5.5: Upper results of the NH₃VAPOR sensitivity analysis. The peak temperature used was 150 °C and, as shown by the vapor fraction (VAPRFRAC) column, the NH₃/water stream keeps a liquid fraction of 1.



Row/Case	Status	VARY 1 MIDTMPXR PARAM TEMP	FSO3	T	FH2
		C	KMOL/HR	C	KMOL/HR
63	Errors	831	5900.38078	831	4830.48202
64	Errors	831.5	5997.04647	831.5	4905.29483
65	Errors	832	6095.00111	832	4981.10484
66	Warnings	832.5	6194.26197	832.5	5057.92577
67	Warnings	833	6294.84656	833	5135.77122
68	Warnings	833.5	6396.77263	833.5	5214.65499
69	OK	834	6500.05817	834	5278.09345
70	OK	834.5	6604.72139	834.5	5278.09398
71	OK	835	6710.78077	835	5278.09468
72	OK	835.5	6818.25504	835.5	5278.09558
73	OK	836	6927.16315	836	5278.09668
74	Errors	836.5	7037.52435	836.5	5278.098
75	Errors	837	7149.35811	837	5278.09946
76	Errors	837.5	7262.6842	837.5	5278.10105

Figure 5.6: Intermediate results of the SO3PROD sensitivity analysis. Displays the range of temperatures where the chosen temperature for the mid-temperature reactor of 834.5 °C is located including examples of the temperature ranges that showed a status of errors or warnings. The column FSO3 is the flow of SO₃, column T is the temperature of the mid-temperature reactor, and column FH2 is the flow of product H₂.

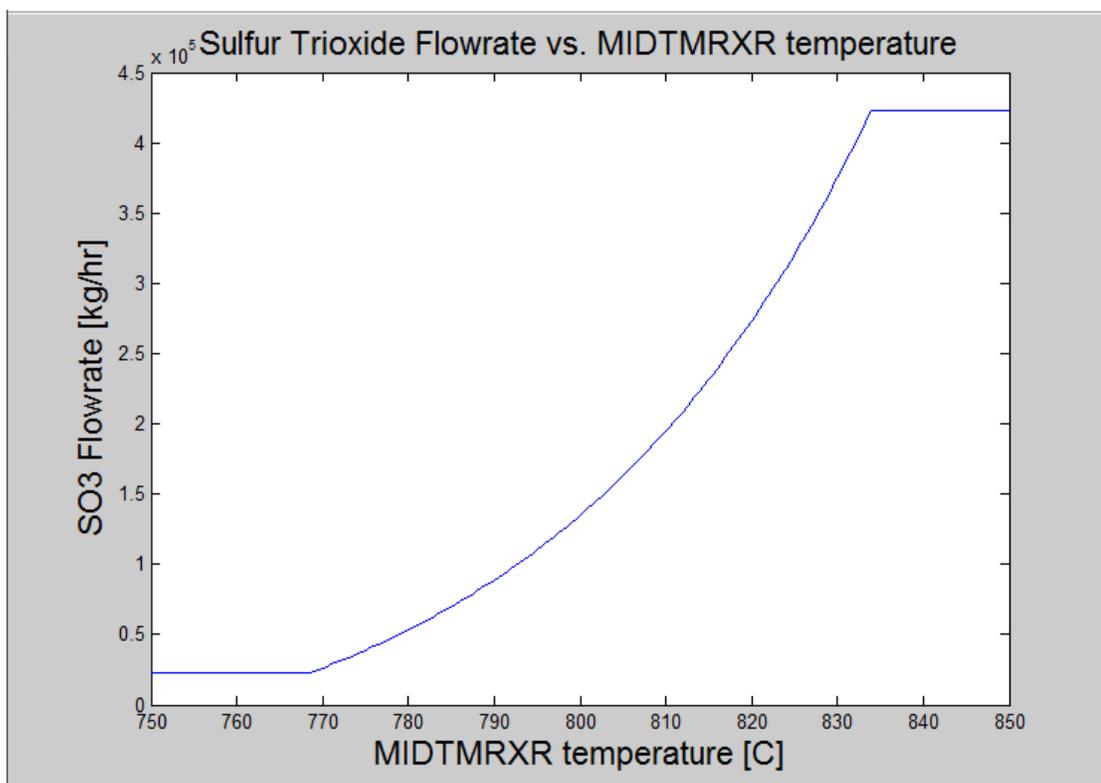


Figure 5.7: Plot of the sensitivity analysis SO3PROD showing the mass flow rate of SO₃ [kg/hr] versus the temperature of the mid-temperature reactor.

References

- [1] Lindberg, D., Backman, R., Chartrand, P., "Thermodynamic Evaluation and Optimization of the (Na₂SO₄ + K₂SO₄ + Na₂S₂O₇ + K₂S₂O₇) System," *Journal of Chemical Thermodynamics*, v.38, **2006**, p. 1568-1583
- [2] Turton, Richard, Richard C. Bailie, Wallace B. Whiting, and Joseph A. Shaeiwitz. *Analysis, Synthesis and Design of Chemical Processes*. Upper Saddle River, NJ: Prentice-Hall, 1998. Print.
- [3] Kemp, Ian C. *Pinch Analysis and Process Integration: A User Guide on Process Integration for the Efficient Use of Energy*. Oxford: Butterworth-Heinemann, 2007. Print.
- [4] Bloch, Heinz P. *Process Plant Machinery*. Boston: Butterworths, 1989. Print.
- [5] Wang, M.K. *Study of the Thermochemistry for Oxygen Production for a Solar Sulfur-Ammonia Water-Splitting Process*. M.S. thesis, University of California, San Diego, 2012.
- [6] "Lower and Higher Heating Values of Fuels." *Hydrogen Data Resource Center: Hydrogen Calculator*. N.p., n.d. Web. 17 July 2012.
http://hydrogen.pnl.gov/cocoon/morf/hydrogen/site_specific/fuel_heating_calculator?canprint=false.

Chapter 6: Conclusions and Future Work

The objective of this study was to determine the overall viability of the sulfur-ammonia solar thermochemical hydrogen production process. This included convergence of the material and energy flows throughout the process, input of laboratory data for more realistic reactor design, pinch analysis and heat integration, electrical generation for the electrolyzer and various other units requiring work, and a suitable efficiency for a preliminary flow sheet.

Table 5.2 showed convergence of the energy and mass balance with a percent difference of 0.07% and 0.00%, respectively. These percent differences are low and within acceptable tolerances because the tolerances allowed in Aspen Plus[®] are stringent. The final flow sheet in Figure 1.3 does converge and it incorporated laboratory results that included phase diagram data of the $K_2S_2O_7/K_2SO_4$ system and enthalpy and Gibbs free energy of the potassium and ammonium salts. To incorporate laboratory data into the flow sheet, a design specification was placed around the mid-temperature reactor to determine a conversion of 0.20 of the potassium pyrosulfate was required at a temperature of 835 °C to produce $5.29E+05$ kg/hr of SO_3 at the system pressure of 9 bar, an excess of what is required to produce the necessary amount of hydrogen. To aid in convergence, another design specification was placed in the flow sheet to determine that an additional 4,200 kg/hr of water was needed as make-up to the plant's only feed stream; due to the losses in the hydrogen product stream.

A pinch analysis was performed to incorporate heat integration so useful energy was not lost. The pinch analysis was a good preliminary point to start

designing a heat exchanger network but the network in the final flow sheet successfully exchanged useful heat to the areas where it was needed the most. A total of 250 MW of energy was transferred between streams.

Electrical generation was accomplished using a single-flow condensing turbine placed in the 400 °C-9 bar ammonia/steam product of the low temperature reactor. This was able to produce 248 MW of electrical power which was sufficient to supply the electrolyzer power requirement of 226 MW.

A calculator block was placed in the flow sheet to determine the overall efficiency of the plant whenever the simulation was conducted and convergence was achieved. Based on the total molar flow rate of 5278 kmol/hr of hydrogen produced, the efficiency of the final flow sheet was found to be 23%.

The simulations performed on the flow sheet designed in this thesis indicate that this thermochemical cycle is thermodynamically viable. Convergence was achieved and laboratory data were both successfully input into the flow sheet and seen as results of the simulation. Although these preliminary results are positive, much more work must be done to create an even more robust and realistic simulation of the plant. Alternate methods of power generation should be researched such as an exterior steam power plant. This would have the added effect of a possible lower system pressure that would need further research to show the effects of this lower pressure. The manual tear streams have the possibility of being closed using more design specifications throughout the process and this would allow the flow sheet to converge completely. The production of hydrogen is slightly lower than the required amount set forth by the DOE. The amount of hydrogen produced is lower than required only

because of scaling. The current flow sheet is easily scalable and can be increased as needed. Research into increasing the ammonia production in the low temperature reactor while maintaining or lowering the heat duty of the reactor may solve the issue.

Future work should also include measurement of the reaction kinetics/mass transfer rates in the low temperature reactor, mid-temperature reactor, and the chemical absorber. A more in depth design of the reactors is required such as their scaling for a more realistic simulation of this process.

This final flow sheet represents a complete preliminary design and, with more research, will become an extremely useful tool in designing scaled hydrogen production plants.

Appendices

A. Electrochemical Relations for ELECPOWR FORTRAN Code

To determine the power requirement of the electrolyzer, electrochemical relations were used to find power in terms of the amount of hydrogen produced and the voltage used in the electrolysis reactor. The following is the derivation of this relation.

$$J \left[\frac{A}{m^2} \right] = \text{current density}$$

$$S[m^2] = \text{electrode area}$$

$$E[V] = E \left[\frac{J}{C} \right] = \text{voltage}$$

$$F = \text{Faraday's constant} = 96,485 \left[\frac{C}{mol} \right]$$

$$z = 2 \text{ (charge needed per mole of } H_2 \text{ released [} 2H^+ + 2e^- \rightarrow H_2 \text{])}$$

$$I[A] = I \left[\frac{C}{s} \right] = J \left[\frac{A}{m^2} \right] S[m^2]$$

$$Q[C] = \text{charge transferred across electrode} = I[A]t[s] = I \left[\frac{C}{s} \right] t[s]$$

$$\text{For } N \text{ [mol/s]}$$

$$\frac{N \text{ mol } H_2}{t[s]} = \frac{I \left[\frac{C}{s} \right]}{F \frac{C}{mol} \cdot z}$$

$$\text{Power [W]} = I[A]E[V] = I \left[\frac{C}{s} \right] E \left[\frac{J}{C} \right] = J \left[\frac{A}{m^2} \right] S[m^2]E[V]$$

For 1 mol H_2 released, $zF[C] = 2F[C]$ charge transferred are needed. For N mol H_2 per second, $zFN[A] = 2FN[A]$ of current is needed. At $J[A/m^2]$

$$S[m^2] = \frac{zFN}{J} [m^2]$$

For N moles H₂ released per second

$$Power[W] = J \left[\frac{A}{m^2} \right] \frac{2FN}{J} [m^2] E[V] = 2FNE[W]$$

This shows the relation between the power requirement and the voltage and number of moles of H₂ produced. This was used in the ELECPOWR calculator block to determine the electrical requirement of the electrolyzer.

B. LHV of Hydrogen Conversion Factor

The defined flow basis for this work was kmol/hr. From the DOE website [1], a conversion factor of 119.96 MJ/kg H₂ was used to determine the LHV of H₂.

Therefore, it follows that

$$\frac{N \text{ kmol } H_2}{hr} \times \frac{2.016 \text{ kg } H_2}{\text{kmol } H_2} \times 119.96 \frac{MJ}{\text{kg } H_2} \times \frac{hr}{3600 s} = 0.0671776N \text{ MW}$$

However, in the instances where this value was used, the units must be correct. There was no unit conversion once this value was used in, for example, a design specification. Therefore, because units of Watts were necessary

$$0.0671776N \text{ MW} \times \frac{10^6 \text{ W}}{1 \text{ MW}} = 67,177.6N \text{ W}$$

where the variable (N) was the amount of hydrogen produced with units of [kmol/hr].

This conversion factor was used to calculate the efficiency of the plant dependent on the amount of hydrogen produced.

C. Complete Stream Tables

C.1 Molar Flow Stream Table

Table C.1.1: Molar flow rate stream table including every stream in the process.

Stream Name	AM2SO4-1	AM2SO4-2	AM2SO422	BOTTOMS	ELECPROD	H2	H2-COMP	H2-H2O	H2O-FEED
To	LOTEMRXR	HX-3		BOTTOMS	ELECFLSH	COMPRESS		H2SEP	MIXER
From		ELECFLSH	HX-3	H2SEP	ELECTROL	H2SEP	COMPRESS	ELECFLSH	
Phase	LIQUID	LIQUID	MIXED	LIQUID	MIXED	VAPOR	VAPOR	VAPOR	LIQUID
Mole Flow kmol/hr									
H2O	46000	45999.08	45999.08	511.8273	46510.9	0	0	511.8273	5789.105
AM2SO3	277.8	277.8	277.8	0	277.8	0	0	1.06E-92	0
AM2SO4	5278.2	5278.2	5278.2	0	5278.2	0	0	1.23E-92	0
K2SO4	0	0	0	0	0	0	0	0	0
K2S2O7	0	0	0	0	0	0	0	0	0
NH3	0	0	0	0	0	0	0	0	0
SO3	0	1215.259	1215.259	9.430418	1224.689	0	0	9.430418	0
SO2	0	101.3212	101.3212	0.528171	101.8494	0	0	0.528171	0
O2	0	0	0	0	0	0	0	0	0
H2SO4	0	0	0	0	0	0	0	0	0
H2	0	0.1059968	0.1059968	0	5278.2	5278.094	5278.094	5278.094	0
NH4+	0	0	0	0	0	0	0	0	0
K+	0	0	0	0	0	0	0	0	0
H3O+	0	0	0	0	0	0	0	0	0
OH-	0	0	0	0	0	0	0	0	0
HSO4-	0	0	0	0	0	0	0	0	0
HSO3-	0	0	0	0	0	0	0	0	0
SO3--	0	0	0	0	0	0	0	0	0
SO4--	0	0	0	0	0	0	0	0	0
Total Flow kmol/hr	51556	52871.76	52871.76	521.7859	58671.64	5278.094	5278.094	5799.88	5789.105

Table C.1.1: Continued.

Stream Name	NH3-W	O2	O2-ATMO	O2PRESS	SFIT-H2O	SFITH2O2	SFITPRD2	SFITPRD3	SFITPROD
To	ABSORBER	O2EXPAND		O2-HEATR	PUMP-1	ELECTROL	HX-4	MIXER	SEP-ABS
From	HX-4	SEP-ABS	O2-HEATR	O2EXPAND	MIXER	PUMP-1	SEP-ABS	HX-4	ABSORBER
Phase	LIQUID	VAPOR	VAPOR	VAPOR	LIQUID	LIQUID	LIQUID	LIQUID	MIXED
Mole Flow kmol/hr									
H2O	51556	0	0	0	51789.11	51789.11	460000	46000	46000
AM2SO3	0	0	0	0	5556	5556	5556	5556	5556
AM2SO4	0	0	0	0	0	0	0	0	0
K2SO4	0	0	0	0	0	0	0	0	0
K2S2O7	0	0	0	0	0	0	0	0	0
NH3	11112	0	0	0	0	0	0	0	0
SO3	0	0	0	0	1224.689	1224.689	1224.689	1224.689	1224.689
SO2	277.8	0	0	0	101.8494	101.8494	101.8494	101.8494	101.8494
O2	0	2690.025	2690.025	2690.025	0	0	0	0	2690.025
H2SO4	0	0	0	0	0	0	0	0	0
H2	0	0	0	0	0	0	0	0	0
NH4+	0	0	0	0	0	0	0	0	0
K+	0	0	0	0	0	0	0	0	0
H3O+	0	0	0	0	0	0	0	0	0
OH-	0	0	0	0	0	0	0	0	0
HSO4-	0	0	0	0	0	0	0	0	0
HSO3-	0	0	0	0	0	0	0	0	0
SO3--	0	0	0	0	0	0	0	0	0
SO4--	0	0	0	0	0	0	0	0	0
Total Flow kmol/hr	62945.8	2690.025	2690.025	2690.025	58671.64	58671.64	52882.54	52882.54	55572.56

Table C.1.1: Continued.

Stream Name	SO2-O2	SO2-O2-2	SO2-O2-3	SO2-O2-4	SO3	SO3-2	VAPRTEST
To	HX-1	ABSORBER	HX-2	HX-3	HITEMRXR	HX-1	TEST
From	HITEMRXR	HX-3	HX-1	HX-2	HX-1	SEP-MID	PUMP-2
Phase	VAPOR	VAPOR	VAPOR	VAPOR	VAPOR	VAPOR	LIQUID
Mole Flow kmol/hr							
H2O	0	0	0	0	0	0	51556
AM2SO3	0	0	0	0	0	0	0
AM2SO4	0	0	0	0	0	0	0
K2SO4	0	0	0	0	0	0	0
K2S2O7	0	0	0	0	0	0	0
NH3	0	0	0	0	0	0	11112
SO3	1224.689	1224.689	1224.689	1224.689	6604.738	6604.738	0
SO2	5380.049	5380.049	5380.049	5380.049	0	0	277.8
O2	2690.025	2690.025	2690.025	2690.025	0	0	0
H2SO4	0	0	0	0	0	0	0
H2	0	0	0	0	0	0	0
NH4+	0	0	0	0	0	0	0
K+	0	0	0	0	0	0	0
H3O+	0	0	0	0	0	0	0
OH-	0	0	0	0	0	0	0
HSO4-	0	0	0	0	0	0	0
HSO3-	0	0	0	0	0	0	0
SO3--	0	0	0	0	0	0	0
SO4--	0	0	0	0	0	0	0
Total Flow kmol/hr	9294.763	9294.763	9294.763	9294.763	6604.738	6604.738	62945.8

C.2 Molar Fraction Stream Table

Table C.2.1: Continued.

Stream Name	SO2-O2	SO2-O2-2	SO2-O2-3	SO2-O2-4	SO3	SO3-2	VAPRTEST
To	HX-1	ABSORBER	HX-2	HX-3	HITEMRXR	HX-1	TEST
From	HITEMRXR	HX-3	HX-1	HX-2	HX-1	SEP-MID	PUMP-2
Phase	VAPOR	VAPOR	VAPOR	VAPOR	VAPOR	VAPOR	LIQUID
Mole Flow kmol/hr							
H2O	0	0	0	0	0	0	0.8190539
AM2SO3	0	0	0	0	0	0	0
AM2SO4	0	0	0	0	0	0	0
K2SO4	0	0	0	0	0	0	0
K2S2O7	0	0	0	0	0	0	0
NH3	0	0	0	0	0	0	0.1765328
SO3	0.1317612	0.1317612	0.1317612	0.1317612	1	1	0
SO2	0.5788259	0.5788259	0.5788259	0.5788259	0	0	4.41E-03
O2	0.2894129	0.2894129	0.2894129	0.2894129	0	0	0
H2SO4	0	0	0	0	0	0	0
H2	0	0	0	0	0	0	0
NH4+	0	0	0	0	0	0	0
K+	0	0	0	0	0	0	0
H3O+	0	0	0	0	0	0	0
OH-	0	0	0	0	0	0	0
HSO4-	0	0	0	0	0	0	0
HSO3-	0	0	0	0	0	0	0
SO3--	0	0	0	0	0	0	0
SO4--	0	0	0	0	0	0	0

C.3 Mass Flow Stream Table

Table C.3.1: Mass flow rate stream table including every stream in the process.

Stream Name	AM2SO4-1	AM2SO4-2	AM2SO422	BOTTOMS	ELECPROD	H2	H2-COMP	H2-H2O	H2O-FEED
To	LOTEMRXR	HX-3		BOTTOMS	ELECFLSH	COMPRESS		H2SEP	MIXER
From		ELECFLSH	HX-3	H2SEP	ELECTROL	H2SEP	COMPRESS	ELECFLSH	
Phase	LIQUID	LIQUID	MIXED	LIQUID	MIXED	VAPOR	VAPOR	VAPOR	LIQUID
Mass Flow kg/hr									
H2O	8.29E+05	8.29E+05	8.29E+05	9220.713	8.38E+05	0	0	9220.713	1.04E+05
AM2SO3	32264.03	32264.03	32264.03	0	32264.03	0	0	1.23E-90	0
AM2SO4	6.97E+05	6.97E+05	6.97E+05	0	6.97E+05	0	0	1.62E-90	0
K2SO4	0	0	0	0	0	0	0	0	0
K2S2O7	0	0	0	0	0	0	0	0	0
NH3	0	0	0	0	0	0	0	0	0
SO3	0	97298.71	97298.71	755.0389	98053.75	0	0	755.0389	0
SO2	0	6491.123	6491.123	33.83717	6524.96	0	0	33.83717	0
O2	0	0	0	0	0	0	0	0	0
H2SO4	0	0	0	0	0	0	0	0	0
H2	0	0.2136768	0.2136768	0	10640.22	10640	10640	10640	0
NH4+	0	0	0	0	0	0	0	0	0
K+	0	0	0	0	0	0	0	0	0
H3O+	0	0	0	0	0	0	0	0	0
OH-	0	0	0	0	0	0	0	0	0
HSO4-	0	0	0	0	0	0	0	0	0
HSO3-	0	0	0	0	0	0	0	0	0
SO3--	0	0	0	0	0	0	0	0	0
SO4--	0	0	0	0	0	0	0	0	0
Total Flow kg/hr	1.56E+06	1.66E+06	1.66E+06	10009.59	1.68E+06	10640	10640	20649.59	1.04E+05

Table C.3.1: Continued.

Stream Name	K2S2O7-2	K2S2O7	K2SO4	K2SO4-2	K2SO4SO3	NH3-C1	NH3-C2	NH3-C3	NH3-HOT
To	MIDTMRXR HX-2	HX-2 LOTEMRXR LIQUID	LOTEMRXR LIQUID	SEP-MID LIQUID	SEP-MID MIDTMRXR MIXED	CONDENSE TURBINE MIXED	PUMP-2 CONDENSE LIQUID	HX-4 TEST LIQUID	TURBINE LOTEMRXR VAPOR
From	HX-2 LIQUID	LOTEMRXR LIQUID	LIQUID	SEP-MID LIQUID	MIDTMRXR MIXED	TURBINE MIXED	CONDENSE LIQUID	TEST LIQUID	LOTEMRXR VAPOR
Phase	LIQUID	LIQUID	LIQUID	LIQUID	MIXED	MIXED	LIQUID	LIQUID	VAPOR
Mass Flow kg/hr									
H2O	0	0	0	0	0	9.29E+05	9.29E+05	9.29E+05	9.29E+05
AM2SO3	0	0	0	0	0	0	0	0	0
AM2SO4	0	0	0	0	0	0	0	0	0
K2SO4	2.42E+05	2.42E+05	1.16E+06	1.39E+06	1.39E+06	0	0	0	0
K2S2O7	8.12E+06	8.12E+06	6.78E+06	6.45E+06	6.45E+06	0	0	0	0
NH3	0	0	0	0	0	1.89E+05	1.89E+05	1.89E+05	1.89E+05
SO3	0	0	0	0	5.29E+05	0	0	0	0
SO2	0	0	0	0	0	17797.2	17797.2	17797.2	17797.2
O2	0	0	0	0	0	0	0	0	0
H2SO4	0	0	0	0	0	0	0	0	0
H2	0	0	0	0	0	0	0	0	0
NH4+	0	0	0	0	0	0	0	0	0
K+	0	0	0	0	0	0	0	0	0
H3O+	0	0	0	0	0	0	0	0	0
OH-	0	0	0	0	0	0	0	0	0
HSO4-	0	0	0	0	0	0	0	0	0
HSO3-	0	0	0	0	0	0	0	0	0
SO3--	0	0	0	0	0	0	0	0	0
SO4--	0	0	0	0	0	0	0	0	0
Total Flow kg/hr	8.37E+06	8.37E+06	7.94E+06	7.84E+06	8.37E+06	1.14E+06	1.14E+06	1.14E+06	1.14E+06

Table C.3.1: Continued.

Stream Name	NH3-W	O2	O2-ATMO	O2PRESS	SFIT-H2O	SFITH2O2	SFITPRD2	SFITPRD3	SFITPROD
To	ABSORBER	O2EXPAND		O2-HEATR	PUMP-1	ELECTROL	HX-4	MIXER	SEP-ABS
From	HX-4	SEP-ABS	O2-HEATR	O2EXPAND	MIXER	PUMP-1	SEP-ABS	HX-4	ABSORBER
Phase	LIQUID	VAPOR	VAPOR	VAPOR	LIQUID	LIQUID	LIQUID	LIQUID	MIXED
Mass Flow kg/hr									
H2O	9.29E+05	0	0	0	9.33E+05	9.33E+05	8.29E+05	8.29E+05	8.29E+05
AM2SO3	0	0	0	0	6.45E+05	6.45E+05	6.45E+05	6.45E+05	6.45E+05
AM2SO4	0	0	0	0	0	0	0	0	0
K2SO4	0	0	0	0	0	0	0	0	0
K2S2O7	0	0	0	0	0	0	0	0	0
NH3	1.89E+05	0	0	0	0	0	0	0	0
SO3	0	0	0	0	98053.75	98053.75	98053.75	98053.75	98053.75
SO2	17797.2	0	0	0	6524.96	6524.96	6524.96	6524.96	6524.96
O2	0	86077.56	86077.56	86077.56	0	0	0	0	86077.56
H2SO4	0	0	0	0	0	0	0	0	0
H2	0	0	0	0	0	0	0	0	0
NH4+	0	0	0	0	0	0	0	0	0
K+	0	0	0	0	0	0	0	0	0
H3O+	0	0	0	0	0	0	0	0	0
OH-	0	0	0	0	0	0	0	0	0
HSO4-	0	0	0	0	0	0	0	0	0
HSO3-	0	0	0	0	0	0	0	0	0
SO3--	0	0	0	0	0	0	0	0	0
SO4--	0	0	0	0	0	0	0	0	0
Total Flow kg/hr	1.14E+06	86077.56	86077.56	86077.56	1.68E+06	1.68E+06	1.58E+06	1.58E+06	1.66E+06

C.4 Heat, Pressure, Phase, and Density Stream Table

Table C-4.1: Stream table including temperature, pressure, vapor fraction, liquid fraction, enthalpy, and density of every stream in the process.

Stream Name	AM2SO4-1	AM2SO4-2	AM2SO422	BOTTOMS	ELECPROD	H2	H2-COMP	H2-H2O	H2O-FEED
To	LOTEMRXR	HX-3		BOTTOMS	ELECFLSH	COMPRESS		H2SEP	MIXER
From		ELECFLSH	HX-3	H2SEP	ELECTROL	H2SEP	COMPRESS	ELECFLSH	
Phase	LIQUID	LIQUID	MIXED	LIQUID	MIXED	VAPOR	VAPOR	VAPOR	LIQUID
Temperature °C	176	100	176	100	130	100	226.247	100	25
Pressure bar	9	9	9	9	9	9	21.7	9	1
Vapor Fraction	0	0	0.0405064	0	0.1181324	1	1	1	1
Liquid Fraction	1	1	0.9594935	1	0.8818676	0	0	0	0
Enthalpy J/kmol	-3.70E+08	-3.75E+08	-3.70E+08	-2.83E+08	-3.37E+08	2.16E+06	5.84E+06	-1.98E+07	-2.86E+08
Enthalpy J/kg	-1.23E+07	-1.19E+07	-1.18E+07	-1.48E+07	-1.18E+07	1.07E+06	2.89E+06	-5.57E+06	-1.59E+07
Enthalpy Watt	-5.30E+09	-5.51E+09	-5.43E+09	-4.10E+07	-5.49E+09	3.16E+06	8.56E+06	-3.20E+07	-4.60E+08
Density kg/cum	679.9583	1215.841	153.66	988.9837	61.81748	0.5820732	1.044304	1.029549	997.1673

Table C.4.1: Continued.

Stream Name	K2S2O7-2	K2S2O7	K2SO4	K2SO4-2	K2SO4SO3	NH3-C1	NH3-C2	NH3-C3	NH3-HOT
To	MIDTMRXR HX-2	LOTEMRXR LIQUID	LOTEMRXR LIQUID	SEP-MID LIQUID	SEP-MID MIDTMRXR MIXED	CONDENSE TURBINE MIXED	PUMP-2 CONDENSE LIQUID	HX-4 TEST LIQUID	TURBINE LOTEMRXR VAPOR
From	HX-2	LOTEMRXR LIQUID	LOTEMRXR LIQUID	SEP-MID LIQUID	MIDTMRXR MIXED	TURBINE MIXED	CONDENSE LIQUID	TEST LIQUID	LOTEMRXR VAPOR
Phase	LIQUID	LIQUID	LIQUID	LIQUID	MIXED	MIXED	LIQUID	LIQUID	VAPOR
Temperature °C	785	400	834.5	834.5	834.5	43.25193	-4.463069	-4.24254	400
Pressure bar	9	9	9	9	9	0.08	0.08	9	9
Vapor Fraction	0	0	0	0	0	0.9724427	0	0	1
Liquid Fraction	1	1	1	1	1	0.0275572	1	1	0
Enthalpy J/kmol	-1.95E+09	-1.95E+09	-1.85E+09	-1.83E+09	-1.59E+09	-2.08E+08	-2.53E+08	-2.53E+08	-1.94E08
Enthalpy J/kg	-7.77E+06	-7.77E+06	-7.77E+06	-7.80E+06	-7.58E+06	-1.15E+07	-1.40E+07	-1.40E+07	-1.08E+07
Enthalpy Watt	-1.81E+10	-1.81E+10	-1.72E+10	-1.70E+10	-1.76E+10	-3.64E+09	-4.42E+09	-4.42E+09	-3.39E+09
Density kg/cum	638.1493	638.1493	504.5084	760.098	107.6044	0.0564743	934.177	934.0875	3.934345

Table C.4.1: Continued.

Stream Name	NH3-W	O2	O2-ATMO	O2PRESS	SFIT-H2O	SFITH2O2	SFITPRD2	SFITPRD3	SFITPRD
To	ABSORBER	O2EXPAND		O2-HEATR	PUMP-1	ELECTROL	HX-4	MIXER	SEP-ABS
From	HX-4	SEP-ABS	O2-HEATR	O2EXPAND	MIXER	PUMP-1	SEP-ABS	HX-4	ABSORBER
Phase	LIQUID	VAPOR	VAPOR	VAPOR	LIQUID	LIQUID	LIQUID	LIQUID	MIXED
Temperature °C	88	162.4273	25	-7.016449	103.1026	103.2839	162.4273	107.6561	162.4273
Pressure bar	9	9	1.01325	1.01325	1	9	9	9	9
Vapor Fraction	0	1	1	1	0	0	0	0	0.1067172
Liquid Fraction	1	0	0	0	1	1	1	1	0.8932828
Enthalpy J/kmol	-2.45E+08	4.08E+06	-8061.021	-9.48E+05	-3.37E+08	-3.37E+08	-3.33E+08	-3.42E+08	-3.14E+08
Enthalpy J/kg	-1.36E+07	1.28E+05	-251.9163	-29610.83	-1.17E+07	-1.17E+07	-1.11E+07	-1.15E+07	-1.05E+07
Enthalpy Watt	-4.28E09	3.05E+06	-6023.429	-7.08E+05	-5.48E+09	-5.48E+09	-4.88E+09	-5.02E+09	-4.85E+09
Density kg/cum	847.9472	7.953535	1.308934	1.467043	925.5722	925.3427	711.2983	911.0789	64.98326

Table C.4.1: Continued.

Stream Name	SO2-O2	SO2-O2-2	SO2-O2-3	SO2-O2-4	SO3	SO3-2	VAPRTEST
To	HX-1	ABSORBER	HX-2	HX-3	HITEMRXR	HX-1	TEST
From	HITEMRXR	HX-3	HX-1	HX-2	HX-1	SEP-MID	PUMP-2
Phase	VAPOR	VAPOR	VAPOR	VAPOR	VAPOR	VAPOR	LIQUID
Temperature °C	1000	145.3806	847.3433	806.7771	980	834.5	-4.24254
Pressure bar	9	9	9	9	9	9	9
Vapor Fraction	1	1	1	1	1	1	0
Liquid Fraction	0	0	0	0	0	0	1
Enthalpy J/kmol	-1.77E+08	-2.20E+08	-1.85E+08	-1.87E+08	-3.29E+08	-3.41E+08	-2.53E+08
Enthalpy J/kg	-3.11E+06	-3.86E+06	-3.25E+06	-3.29E+06	-4.11E+06	-4.25E+06	-1.40E+07
Enthalpy Watt	-4.57E+08	-5.67E+08	-4.78E+08	-4.83E+08	-6.04E08	-6.25E+08	-4.42E+09
Density kg/cum	4.833634	15.13192	5.494559	5.701923	6.921134	7.839147	934.0875

References

- [1] "Lower and Higher Heating Values of Fuels." *Hydrogen Data Resource Center: Hydrogen Calculator*. N.p., n.d. Web. 17 July 2012.
http://hydrogen.pnl.gov/cocoon/morf/hydrogen/site_specific/fuel_heating_calculator?canprint=false.